Nuclear Safety
NEA/CSNI/R(2021)8
August 2023
www.oecd-nea.org

OECD/NEA THAI-3 Project Final Report on Fission Product Behaviour, Hydrogen Mitigation, and Hydrogen Combustion in Water Cooled Reactors under Severe Accident Conditions

OECD
BETTER POLICIES FOR BETTER LIVES

NEA
NUCLEAR ENERGY AGENCY

Nuclear Energy Agency

NEA/CSNI/R(2021)8

Unclassified English text only

2 August 2023

NUCLEAR ENERGY AGENCY
COMMITTEE ON THE SAFETY OF NUCLEAR INSTALLATIONS

OECD/NEA THAI-3 Project Final Report on Fission Product Behaviour, Hydrogen Mitigation, and Hydrogen Combustion in Water Cooled Reactors under Severe Accident Conditions

This document is available in PDF format only.

JT03523942

ORGANISATION FOR ECONOMIC CO-OPERATION AND DEVELOPMENT

The OECD is a unique forum where the governments of 38 democracies work together to address the economic, social and environmental challenges of globalisation. The OECD is also at the forefront of efforts to understand and to help governments respond to new developments and concerns, such as corporate governance, the information economy and the challenges of an ageing population. The Organisation provides a setting where governments can compare policy experiences, seek answers to common problems, identify good practice and work to co-ordinate domestic and international policies.

The OECD member countries are: Australia, Austria, Belgium, Canada, Chile, Colombia, Costa Rica, the Czech Republic, Denmark, Estonia, Finland, France, Germany, Greece, Hungary, Iceland, Ireland, Israel, Italy, Japan, Korea, Latvia, Lithuania, Luxembourg, Mexico, the Netherlands, New Zealand, Norway, Poland, Portugal, the Slovak Republic, Slovenia, Spain, Sweden, Switzerland, Türkiye, the United Kingdom and the United States. The European Commission takes part in the work of the OECD.

OECD Publishing disseminates widely the results of the Organisation's statistics gathering and research on economic, social and environmental issues, as well as the conventions, guidelines and standards agreed by its members.

NUCLEAR ENERGY AGENCY

The OECD Nuclear Energy Agency (NEA) was established on 1 February 1958. Current NEA membership consists of 34 countries: Argentina, Australia, Austria, Belgium, Bulgaria, Canada, the Czech Republic, Denmark, Finland, France, Germany, Greece, Hungary, Iceland, Ireland, Italy, Japan, Korea, Luxembourg, Mexico, the Netherlands, Norway, Poland, Portugal, Romania, Russia (suspended), the Slovak Republic, Slovenia, Spain, Sweden, Switzerland, Türkiye, the United Kingdom and the United States. The European Commission and the International Atomic Energy Agency also take part in the work of the Agency.

The mission of the NEA is:

– to assist its member countries in maintaining and further developing, through international co-operation, the scientific, technological and legal bases required for a safe, environmentally sound and economical use of nuclear energy for peaceful purposes;

– to provide authoritative assessments and to forge common understandings on key issues as input to government decisions on nuclear energy policy and to broader OECD analyses in areas such as energy and the sustainable development of low-carbon economies.

Specific areas of competence of the NEA include the safety and regulation of nuclear activities, radioactive waste management and decommissioning, radiological protection, nuclear science, economic and technical analyses of the nuclear fuel cycle, nuclear law and liability, and public information. The NEA Data Bank provides nuclear data and computer program services for participating countries.

COMMITTEE ON THE SAFETY OF NUCLEAR INSTALLATIONS (CSNI)

The Committee on the Safety of Nuclear Installations (CSNI) addresses Nuclear Energy Agency (NEA) programmes and activities that support maintaining and advancing the scientific and technical knowledge base of the safety of nuclear installations.

The Committee constitutes a forum for the exchange of technical information and for collaboration between organisations, which can contribute, from their respective backgrounds in research, development and engineering, to its activities. It has regard to the exchange of information between member countries and safety R&D programmes of various sizes in order to keep all member countries involved in and abreast of developments in technical safety matters.

The Committee reviews the state of knowledge on important topics of nuclear safety science and techniques and of safety assessments, and ensures that operating experience is appropriately accounted for in its activities. It initiates and conducts programmes identified by these reviews and assessments in order to confirm safety, overcome discrepancies, develop improvements and reach consensus on technical issues of common interest. It promotes the co-ordination of work in different member countries that serve to maintain and enhance competence in nuclear safety matters, including the establishment of joint undertakings (e.g. joint research and data projects), and assists in the feedback of the results to participating organisations. The Committee ensures that valuable end-products of the technical reviews and analyses are provided to members in a timely manner, and made publicly available when appropriate, to support broader nuclear safety.

The Committee focuses primarily on the safety aspects of existing power reactors, other nuclear installations and new power reactors; it also considers the safety implications of scientific and technical developments of future reactor technologies and designs. Further, the scope for the Committee includes human and organisational research activities and technical developments that affect nuclear safety.

Foreword

The Organisation for Economic Co-operation and Development (OECD) Nuclear Energy Agency (NEA) launched the THAI-3 (Thermal-hydraulics, Hydrogen, Aerosols and Iodine) project in 2016 as a follow-up to the THAI-2 project. The THAI-3 project aimed to investigate open questions on hydrogen and fission product issues, with special emphasis on hydrogen passive autocatalytic recombiner performance, hydrogen deflagration behaviour, fission product re-entrainment and resuspension behaviour under accident conditions in the containment of water cooled reactors at the extended THAI+ plant at Becker Technologies in Eschborn, Germany.

With an international partnership of more than 20 organisations from 16 countries, the experimental database produced during the project provides valuable support for validation and further development of lumped parameter and computational fluid dynamics approaches based severe accident codes.

Furthermore, the project contributed to the national competence and expertise in the field of reactor safety in NEA member countries and promoted international co-operation between them.

The authors of the present project's final summary report are:

S. Gupta, G. Poss, M. Freitag, E. Schmidt, M. Colombet, B. von Laufenberg, A. Kühnel and G. Langer, all from Becker Technologies GmbH, and F. Funke and G. Langrock, both of Framatome GmbH.

The report was reviewed by the project participants and approved by the NEA Committee on the Safety of Nuclear Installations (CSNI) in December 2020.

Becker Technologies acknowledges the support provided by the NEA during execution of the project. Furthermore, the financial support and technical input provided by all THAI-3 project partners is gratefully acknowledged.

Executive summary

Background

Despite significant improvements in computer codes, there are still deficiencies in modelling certain phenomena related to hydrogen and fission product behaviour during severe accidents in containments of water cooled reactors. In this context, the realistic boundary conditions employed in experiments to validate the concerned computer models play a significant role by providing a reliable basis for containment safety analysis. Uncertainties still exist in the modelling of slow hydrogen deflagration and passive autocatalytic recombiner (PAR) performance behaviour under severe accident conditions. Regarding fission product remobilisation behaviour, the outcomes of Fukushima Daiichi accident analyses (e.g. the NEA BSAF and BSAF-2 projects) have revealed uncertainties during the late phase of the accident, where small but long-term release of fission products may play a vital role in determining the source term to the environment. The experimental investigations carried out in the framework of the NEA THAI-3 project aim to resolve some of the remaining issues related to hydrogen and fission products with specific emphasis on PAR performance, hydrogen deflagration behaviour, and fission product remobilisation behaviour from water pools and surfaces. The aim of carrying out such coupled-phenomena experiments in the framework of an international programme is twofold: to enhance confidence in the performance of safety and mitigation systems during severe accidents; and to establish a common database accessible by a large research community to support further development and validation of lumped parameter (LP) and computational fluid dynamics (CFD) codes.

The NEA THAI-3 project was conducted from 1 February 2016 until 31 July 2019 under the auspices of the Nuclear Energy Agency (NEA). The project was supported by the signatories from Belgium, Canada, China, the Czech Republic, Finland, France, Germany, Hungary, India, Japan, Korea, Luxembourg, the Slovak Republic, Sweden, Switzerland and the United Kingdom. Becker Technologies GmbH acted as operating agent.

Objective of the work

The overall objective of the NEA THAI-3 project was to address open questions concerning the behaviour of hydrogen, iodine and aerosols under severe accident conditions in the containment of water cooled reactors. Understanding the processes taking place during such events is essential to evaluating the challenge posed on containment integrity (due to hydrogen combustion) and for evaluating the amount of airborne radioactivity (iodine and aerosols) during such severe accidents with core damage and the associated source term.

The project also aimed to contribute to the validation and further development of advanced LP- and CFD- codes used for reactor applications, e.g. by providing experimental data for code benchmark exercises. Furthermore, the project aimed to maintain and extend the competence and expertise in the field of reactor safety in the NEA member countries and to promote international co-operation between these countries.

Work performed

Tests were performed in the technical-scale THAI$^+$ containment test facility, which consists of the original THAI vessel (TTV), to which a smaller vessel, designated as a parallel attachable drum (PAD), is interconnected by a lower and upper DN500 pipe. The facility is operated by Becker Technologies GmbH in Eschborn, Germany, under the sponsorship of the German Federal Ministry for Economic Affairs and Energy.

Within the NEA THAI-3 project, the following test series have been performed:

- Hydrogen deflagration tests in two-vessel geometry (HD 40-45);
- Hydrogen PAR tests (HR 46-50);
- Soluble and gaseous fission product (CsI, iodine) release from a boiling pool (WH-24 and WH-28, Iod-32);
- Resuspension of iodine from decontamination paint by H_2 deflagration (Iod-34);
- Resuspension of aerosol deposits from surfaces by hydrogen deflagration (HD-46).

Furthermore, two HD tests (HD-36 and HD-38) and one HR test (HR-43) conducted in the framework of the THAI National (phase V) project have been shared with the NEA THAI-3 project partners at no additional cost.

Extensive analysis by partners in the framework of the Analytical Working Group (AWG) accompanied the experimental programme.

Results

Hydrogen deflagration tests (HD 40-45) in multi-compartment geometry

The hydrogen deflagration test series investigated the effects of superimposed flow on flame propagation. These effects are generally not considered in the existing models and need to be quantified, creating experimental databases for further modelling efforts. Furthermore, the tests addressed the effects of hydrogen deflagrations in a two-vessel configuration, including stratifications of gas concentration and gas temperature. The peak pressures measured in all HD tests remained clearly below the adiabatic isochoric complete combustion (AICC) pressures. The pressure increase gradient does not differ markedly for the single vessel and the two-vessel configuration. Flame acceleration and combustion modes similar to jet ignition were also observed in this test series.

Hydrogen passive autocatalytic recombiner tests (HR 46-50)

An operating PAR subjected to counter-current flow conditions as may typically occur in individual compartments of the containment of a nuclear power plant was the subject of investigation in tests HR-46 to HR-50 by using AREVA and NIS PARs. The counter-current flow velocity was up to 1 m/s in the PAR outlet vicinity. The test results indicate that the PAR with top cover on the chimney and lateral outlets provided effective means to protect the PAR from intrusion of counter-current flow within the range of investigated conditions. The impact of chimney height on PAR performance under counter-current flow conditions was also quantified.

Soluble fission product (CsI, Iodine) release from a boiling pool (WH-24, WH-28, Iod-32)

Three tests were conducted to investigate wet resuspension or re-entrainment of aerosols (WH-24 and WH-28), and release of volatile gaseous iodine (Iod-32) from a water pool under boiling conditions. As compared to test WH-24, which was conducted with de-mineralised water, test WH-28 was conducted with surfactants reducing the surface tension of the water. The aerosol entrainment in the WH-28 test was about one order of magnitude higher compared to test WH-24. Results from different particle measurement techniques that have been used to evaluate the entrainment in tests WH-24 and WH-28, indicate that the absolute entrainment is subject to an uncertainty by a factor of 2 - 5.

Test Iod-32 investigated the release of volatile iodine from a subcooled and boiling sump. Under boiling conditions, the I_2 concentration in the gas was higher by a factor of 100 compared to the end of the reference phase. However, this value has to be considered carefully for reactor application as the conditions of test Iod-32 could influence this result. The adsorption/desorption of I_2 from the steel walls in the PAD gas atmosphere might influence this result as well as the suspected stratification of the gaseous phase just above the sump-gas interface, whose effect would be to underestimate the iodine gaseous concentration in non-boiling conditions.

Resuspension of iodine from painted surfaces by hydrogen deflagration (Iod-34)

Test Iod-34 was aimed at studying the resuspension of iodine from painted surfaces by a hydrogen deflagration. The H_2 deflagration induced a significant iodine release from the surfaces to the gas phase. The iodine release fraction amounts to a range between 4 and 9%, considering experimental uncertainties of the initial iodine loadings on the painted and steel surfaces. Out of the total resuspended amount, 50% of the iodine released by H_2-deflagration is in the form of gaseous organic iodide. The persistent iodine aerosol concentration after deflagration indicates very fine particles. The release of iodine from paint in aerosol form due to hydrogen deflagration is a new path for iodine containment codes. The paint degradation probably also changes the conditions and the mechanism for thermal release of volatile organic iodide from paint. Modelling improvements towards estimation of reliable release of volatile organic iodide from paint are considered necessary for extrapolating to deflagration-relevant temperatures. The investigated iodine release mechanism due to H_2-deflagration indicates complex behaviour (e.g. interaction of released iodine with fresh or degraded paint) and the associated uncertainties may be subject to future experimental work.

Aerosol resuspension by hydrogen deflagration (HD-46)

The objective of test HD-46 was to study the resuspension of aerosols that have been deposited on vertical, horizontal and containment typical step grating surfaces and the thermal decomposition of CsI particles by hydrogen deflagration. Among other effects, resuspension may result in an increase in aerosol concentrations in the containment atmosphere, which in turn may have an influence on the source term from containment to the environment, if an accident management measure such as containment venting is considered. The hydrogen deflagration resuspended about 4% of the previously deposited CsI. The resuspended particles settled at much slower velocity due to the sub-micron range of particle sizes. The release of gaseous iodine by thermal decomposition of CsI particles due to the high temperatures during hydrogen deflagration was measured in the range of about 2%.

Analytical activities

An extensive analytical effort accompanied the experimental programme, consisting of code calculations to support test design, for pre-test assessments, result evaluation and extrapolation to reactor conditions. Data on fission product release from boiling pools and on fission product remobilisation from surfaces due to hydrogen combustion offer a unique database to assess in containment airborne radioactivity during a severe accident. Data on fission product release from boiling pools have been used in severe accident code calculations of the Fukushima Daiichi Nuclear Power Plant accident in the assessment of continued releases in the days following the accident.

Two code benchmark exercises have been conducted during the project. For this purpose, experimental data of a hydrogen deflagration test (HD-44) and of a hydrogen recombiner test (HR-49) were selected for blind and open post-test calculations.

Conclusions and recommendations

The NEA THAI-3 project as a continuation of the THAI-2 project has extended the knowledge and data base of severe accident-related issues. As regards PAR, further data about its behaviour under counter-current flow conditions have been obtained, which allows for better assessment of hydrogen mitigation measures and implementation of appropriate models in accident analysis codes. The tests regarding hydrogen deflagration behaviour in the two-vessel geometry provide data for a sound safety-related assessment of flame acceleration and pressure increase in multi-compartment geometry. The tests concerning both molecular and aerosol-bound iodine release from a boiling sump provide valuable data for the quantification of a potential accident source term. This refers also to the resuspension of iodine from paint and the resuspension of pre-deposited aerosols in the course of a hydrogen deflagration. The database developed in the framework of the NEA THAI-3 project has been and will be extensively used for improvement, further development and validation of LP and CFD codes applied in reactor safety analysis, increasing confidence in these tools.

Remaining open questions with a specific focus on the late phase of a severe accident will be further addressed in upcoming projects. The issues proposed are related to investigations on PAR performance, and PAR interactions with iodine oxides (IOx) and nuclear background aerosol. With respect to hydrogen behaviour, experiments are planned on combustion and flame propagation in a H_2-CO containing atmosphere. Concerning source term related issues, studies are planned on the retention of fission products in a water pool under pool-scrubbing conditions and the IOx behaviour in containment atmosphere including interaction with “nuclear background aerosol” and the thermal stability of IOx. The NEA THEMIS project is currently being conducted to consider the aforementioned issues.

List of abbreviations and acronyms

AERB	Atomic Energy Regulatory Board (India)
AICC	Adiabatic isochoric complete combustion
AWG	Analytical Working Group
BARC	Bhabha Atomic Research Centre (India)
BSAF	Benchmark Study of the Accident at the Fukushima Daiichi Nuclear Power Station
BWR	Boiling water reactor
CFD	Computational fluid dynamics
COCOSYS	COntainment COde SYStem
CSNI	Committee on the Safety of Nuclear Installations (NEA)
EPRI	Electric Power Research Institute (United States)
FTIR	Fourier-transform infrared spectroscopy
GRS	Gesellschaft für Anlagen- und Reaktorsicherheit (Germany)
GS	Gas scrubber
HD	Hydrogen deflagration test
HR	Hydrogen passive autocatalytic recombiner test
IRSN	Institut de Radioprotection et de Sûreté Nucléaire (France)
KAERI	Korea Atomic Energy Research Institute
KHNP	Korea Hydro and Nuclear Power Co., Ltd
KIT	Karlsruhe Institute of Technology (Germany)
LP	Lumped parameter
METUSA	Minimal encroaching turnable stream-wise anemometers
MMD	Mass median diameter
NEA	Nuclear Energy Agency
NIS	NIS Ingenieurgesellschaft MBH (Germany)
NUBIKI	Nuclear Safety Research Institute (Hungary)
OECD	Organisation for Economic Co-operation and Development
PAD	Parallel attachable drum
PAR	Passive autocatalytic recombiner
PWR	Pressurized water reactor
QLR	Quick Look Reports
SSM	Strålsäkerhetmyndigheten (Sweden)
THAI	Thermal-hydraulics, Hydrogen, Aerosols and Iodine

TTV	THAI test vessel
VTT	Teknologian Tutkimuskeskus VTT Oy (Finland)

Table of contents

Tables

Figures

1. Introduction

Over the past fifteen years, THAI experimental data have been continuously used for the validation and development of containment safety analysis tools with a specific focus on severe accident conditions. Significant progress in measuring spatial hydrogen distributions, slow hydrogen deflagration behaviour, performance of PARs under accident conditions, and fission product distribution and interaction with operating safety devices has been achieved with the THAI test facility. Improved models based on THAI experimental data have demonstrated reliable simulations of complex experiments, e.g. hydrogen distribution (NEA THAI HM-2 code benchmark), hydrogen combustion behaviour (ISP-49), and hydrogen recombiner performance (NEA THAI-2 HR-35 benchmark).

Despite significant improvements in available computer codes, there are still deficiencies in modelling certain phenomena. In this context, the realistic boundary conditions employed in experiments to validate the concerned computer models play a significant role by providing a reliable basis for containment safety analysis. Uncertainties still exist in the modelling of slow hydrogen flame propagation in compartmentalised geometries for which not much experimental data at technical/large scale facilities are available in open literature. In particular, the effects of superimposed flow conventions on the flame propagation are generally not considered in the existing models and require quantification of their influence and experimental database for further modelling efforts.

Code validation and development work based on previous THAI/PAR tests under natural convection flow conditions and varying containment atmosphere (e.g. O_2 lean or O_2 rich) demonstrated significant progress towards PAR performance analysis and their response to severe accident conditions. Nevertheless, studies of representative accident sequences indicate that performance of PARs might be affected by adverse flow conditions, e.g. counter-current flow. Therefore, an experimental database related to PAR onset and PAR performance (H_2 recombination rate, H_2 depletion efficiency) under counter-current flow conditions is required to be investigated in order to enhance the predictive capabilities of safety analysis tools.

Regarding open issues related to fission products, environmental measurements made during the Fukushima Daiichi Nuclear Power Plant accident revealed that a significant amount of radionuclides was released into the environment. However, estimates of this released amount proved uncertain not only due to limited knowledge about the accident scenario but also because of uncertainties in quantifying fission product retention and release from water pools under accident conditions. Relatively larger uncertainties were observed during the late phase of the accident, where small but long-term release sources of fission products may play a vital role in determining source term to the environment. The need for a more comprehensive understanding of fission product release from water pools was emphasised by post-Fukushima analysis carried out by individual organisations or in the framework of international projects, e.g. NEA BSAF (NEA, 2016). Particular interest has centred on an experimental database for (soluble/non-soluble) aerosols as well as gaseous iodine re-entrainment from water pools under different thermal conditions (e.g. subcooled, boiling), chemical boundary conditions and the characteristics of release gas into the water pool (e.g. mass flow, non-condensable gas fraction). Another open issue related to source term was to quantify the resuspension behaviour of aerosols and gaseous iodine pre-deposited over containment surfaces. Fission product resuspension may influence the “delayed” source term from containment to the environment, in case of

containment breach or if an accident management measure such as containment venting is considered.

To resolve the remaining open issues, the NEA THAI-3 project focuses on hydrogen and fission product issues with a special emphasis on PAR performance, hydrogen deflagration behaviour, and fission product remobilisation behaviour from water pools and surfaces. The need to carry out such coupled phenomena experiments in the framework of an international programme is twofold: to enhance confidence in the performance of passive mitigation systems during severe accident scenarios and to establish a common database accessible by a large research community to support further development and validation of LP and CFD codes.

The NEA THAI-3 project was conducted from 1 February 2016 until 31 July 2019 under the auspices of the OECD Nuclear Energy Agency. The tests were performed in the technical-scale THAI/THAI$^+$ test facility (two stainless steel vessels, with total volume of 80 m^3) with exchangeable internals for multi-compartment investigations. The THAI/THAI$^+$ test facility is designed for a maximum overpressure of 1.4 MPa at 180 °C and can withstand moderate hydrogen deflagrations. Experiments were performed by use of representative aerosol, iodine and H_2 concentrations and thermal hydraulic conditions. Spatio-temporal fission product behaviour was studied by use of the radiotracer I-123.

The NEA THAI-3 project was supported by the signatories, i.e. safety organisations and research laboratories from 15 countries (see Table 1.1) and received technical contributions from the German partners as listed in Table 1.2.

Table 1.1. NEA THAI-3 signatories

Signatories	Country
The Bel V	Belgium
The Canadian Nuclear Laboratory (CNL)	Canada
The State Nuclear Power Software Development Centre (SNPSDC)	China
The ÚJV Rež, a. s. Czech Republic	Czech Republic
The Teknologian tutkimuskeskus VTT Oy	Finland
The Institut de Radioprotection et de Sûreté Nucléaire (IRSN) jointly with Electricité de France (EDF)	France
Gesellschaft für Anlagen- und Reaktorsicherheit (GRS) gGmbH Becker Technologies GmbH	Germany
The Nuclear Safety Research Institute (NUBIKI), jointly with the MVM Paks Nuclear Power Plant Ltd.	Hungary
The Atomic Energy Regulatory Board (AERB) jointly with the Bhabha Atomic Research Centre (BARC), and the Nuclear Power Corporation of India Ltd. (NPCIL)	India
Nuclear Regulation Authority (NRA)	Japan
The Korea Atomic Energy Research Institute (KAERI) jointly with Korea Hydro and Nuclear Power Co., Ltd (KHNP) and Korea Institute of Nuclear Safety (KINS)	Korea
Ministère de l'Enseignement Supérieur et de la Recherche (MESR)	Luxembourg
Nuclear Regulatory Authority of the Slovak Republic (ÚJD SR)	Slovak Republic
The Strålsäkerhetmyndigheten (SSM)	Sweden
Paul Scherrer Institut (PSI)	Switzerland
Office for Nuclear Regulation (ONR)	United Kingdom

Table 1.2. German Partners in the NEA THAI-3 Project

Project partners	City
Becker Technologies GmbH (operating agent)	Eschborn
Framatome GmbH	Erlangen
RUB Ruhr-Universität-Bochum	Bochum
Gesellschaft für Anlagen- und Reaktorsicherheit (GRS) gGmbH	Cologne
Karlsruhe Institute of Technology (KIT)	Karlsruhe

The operating agent was supported by Framatome's Radiochemical Laboratory, Erlangen, Germany, to operate the iodine instrumentation, to perform chemical analyses, and to evaluate and assess the iodine results.

The contributions provided by GRS, RUB and KIT included design calculations and post-test calculations with the respective codes.

Table 1.3 provides the details of the test matrix designed to improve insight into issues related to hydrogen and fission products. In addition to the experimental work, an accompanying analytical working group (AWG) was established with voluntary technical contributions from project partners in the framework of the NEA THAI-3 project. The AWG aimed at performing design calculations, the evaluation of the test results for further development, blind and open code benchmarks, and validation of the predictive capabilities of advanced LP- and CFD codes currently applied in reactor safety. For this purpose, experimental data of a hydrogen deflagration test (HD-44) and of a hydrogen recombiner test (HR-49) have been selected for blind and open post-test calculations in the framework of NEA THAI-3 benchmark exercises (Freitag and Sonnekalb, 2018), (Freitag and Sonnekalb, 2019).

Furthermore, two HD tests (HD-36 and HD-38) and one HR test (HR-43) conducted in the framework of the THAI National (phase V) project have been shared with the NEA THAI-3 project partners at no additional cost (Gupta et al., 2017), (Freitag et al., 2016), (Freitag et al., 2017c).

Table 1.3. Test matrix developed for the NEA THAI-3 project

Test series/ Test no.	Test series/test designation	No. of tests	Objectives
1	HD Tests (HD 40 - 45): Hydrogen deflagration and flame propagation in two-compartment system	6	Influence of convective flows on flame propagation. Influence of scale on flame acceleration effects. Influence of two-compartment configuration on deflagration behavior. Influence of stratification of gas concentrations and temperature. Comparison to single-compartment tests.
2	HR Tests (HR 46 - 50): Recombiner behaviour	5	Behaviour of two different commercial PAR units under counter-current and natural convection flow conditions. To validate codes on the available experimental database and to evaluate the influence of counter-current flow on PAR performance. To evaluate the influence of the chimney height onto the self-induced PAR flow under counter-current flow. Comparison to single-compartment tests.

Table 1.3. Test matrix developed for the NEA THAI-3 project (Continued)

Test series/ Test no.	Test series/test designation	No. of tests	Objectives
3	WH-Tests (WH-24 and WH-28): Re-entrainment of fission products from water pools	2	Quantify the re-entrainment of soluble fission product CsI from water pools at elevated temperature. Investigate the effect of surface tension on the re-entrainment of CsI from the pool. Contribute to the validation and further development of dedicated empirical or semi-mechanistic models of advanced LP- and CFD codes.
4	Test Iod-32: Volatile Iodine release from boiling water pool	1	Quantification of gaseous iodine release from a boiling water pool for different boiling rates and different pH-values.
5	Test Iod-34: Iodine resuspension by hydrogen deflagration	1	Quantification of resuspension of iodine from painted surfaces pre-loaded with iodine in a representative manner by hydrogen deflagration. Degradation of paint by H_2-deflagration.
6	Test HD-46: Aerosol resuspension and thermal decomposition by hydrogen deflagration	1	Quantification of CsI-aerosol resuspension and its thermal decomposition to gaseous I_2 in high-temperature environment of a hydrogen deflagration.

The experimental data obtained from the different test series demonstrated the capability of the THAI/THAI$^+$ facility to produce high quality, high resolution data on the issues mentioned in Table 1.3. The tests provide a better physical understanding and data for the validation and further development of analytical tools related to:

- The phenomenology of hydrogen deflagration in a two-vessel geometry with interacting flame fronts. The tests provide a comprehensive database for further development and validation of combustion models implemented in containment system codes. Test conditions and parameters were defined considering severe accident thermal hydraulic conditions. For the tests, initial conditions were set to 1.5 bar pressure, 90 °C temperature, 10 vol.-% H_2 concentration and 25 vol.-% steam concentration in premixed gas atmosphere, and up to 12 vol.-% hydrogen concentration in stratified atmosphere. The test parameters that varied were burn direction (upward or downward), initial turbulence, initial gas flow velocities and steam- and temperature stratification.
- The behaviour of two commercially available PAR units (AREVA and NIS) under different flow conditions, e.g. counter-current flow, superimposed natural and forced convection, chimney height effect. The parameters that varied were pressure and temperature. The test series evaluate the influence on PAR performance of the different initial flow conditions as may exist in a multi-compartment geometry, including onset of recombination, recombination rate and H_2 depletion efficiency, effect of initial pressure and temperature on PAR performance.
- The re-entrainment of dissolved CsI from a heated/boiling pool by injection of air and steam/air mixtures using a down-scaled DN 100 downcomer pipe in the test WH-24. Droplets with dissolved CsI evaporate in a superheated atmosphere, and particles are measured (for concentration, size distribution) with various techniques. Particle re-entrainment from a flashing pool, induced by vented depressurisation, is investigated. In test WH-24, de-mineralised water was used and in test WH-28 a surfactant was added to reduce the surface tension of the water. The corresponding test Iod-32 was performed with gaseous iodine being released from a heated/boiling pool.

- The resuspension of iodine from painted surfaces through the impact of a hydrogen deflagration, where the vessel surfaces and the installed painted surfaces were pre-loaded with gaseous iodine, was the subject of test Iod-34. Hydrogen deflagration induces a short but strong impact through high temperatures and high atmospheric flow speeds. Iodine measurements in the test vessel were to be performed to determine the rate and efficiency of I_2 deposition on painted surfaces, the speciation of the released iodine (iodine in aerosol form, molecular iodine, organic iodide), and the degradation of the paint.
- Test HD-46 studied the resuspension by hydrogen deflagration of aerosols that have been deposited on vertical and horizontal surfaces and containment typical step gratings. Furthermore, the test investigated the release of gaseous iodine by thermal decomposition of CsI particles due to the hydrogen deflagration. Both are of interest for long-term fission product behaviour and, hence, for the radiological source term.

For the majority of the experiments, design calculations were performed by the operating agent for the detailed determination of test conditions, test parameters, and test procedures and for the detailed design and configuration of the instrumentation and other experimental equipment.

Numerous analytical activities with respect to the tests are documented in the respective reports and publications. The AWG of NEA THAI-3 project organised two code benchmark exercises; one based on the hydrogen deflagration test HD-44 and the second based on PAR performance test HR-49. The code benchmark exercise for HD-44 and HR-49 tests included both Blind-phase and Open-phase calculations, the results of which are documented in the respective comparison reports, namely (Freitag and Sonnenkalb, 2019) and (Freitag and Sonnenkalb, 2018). In addition to HD-44 and HR-49, other tests from the hydrogen deflagration and PAR performance test series have also been used extensively by a majority of the project partners for code-model validation purposes.

For the fission product re-entrainment tests (WH-24, WH-28 and Iod-32), and fission product resuspension tests Iod-34 and HD-46, post-test calculations were performed by the partners and some of results were reported at the AWG meetings, e.g. by IRSN, GRS, VTT. The THAI re-entrainment experimental results also provided feedback in an IRSN analysis performed to study the impact of aerosol re-entrainment from pressure suppression pools on the source term of the Fukushima Daiichi Nuclear Power Plant accident with ASTEC.

The experimental results obtained in the framework of the present experimental programme have helped to achieve the goals of the NEA THAI-3 project, namely to improve confidence in available LP- and CFD-tools for containment analysis. The enhanced tools validated against experimental data will provide a more reliable approach for the analysis of the containment response during accidents and the planning of accident management measures.

The data of all the performed experiments have been processed, qualified and stored on a server hosted by the NEA and are accessible to signatory partners. Detailed experimental results and analyses are provided in Quick Look Reports (QLR) and Technical Reports. The Management Board of the THAI-3 Project has agreed that these QLR and Technical Reports can be disclosed for non-signatory NEA countries after 31 July 2023 and may be obtained after this date upon request from the NEA Secretariat. These reports are compiled in Annex A of this report.

2. Objectives

The overall objective of the NEA THAI-3 project was to address open questions concerning the behaviour of hydrogen, iodine and aerosols in the containment of water cooled reactors during severe accidents. The understanding of the processes taking place during such events is essential for evaluating the challenge posed on containment integrity (by hydrogen combustion) and for evaluating the amount of airborne radioactivity (iodine and aerosols) during such severe accidents with core damage. The project generated valuable data for evaluating the hydrogen deflagration behaviour in a multi-compartment geometry with interacting flame fronts and its effective removal by PARs. Concerning fission products, the project focused on the resuspension of iodine from a painted surface and aerosols deposited on surfaces including containment typical gratings by a hydrogen deflagration and on the release of volatile iodine and soluble aerosol from a boiling pool. Extensive analytical effort accompanied the experimental programme consisting of code calculations to support test design for pre-test assessments, result evaluation and extrapolation to reactor conditions.

The project contributed to the validation and further development of advanced LP- and CFD codes used for reactor applications by for example, providing experimental data for code benchmark exercises. Furthermore, the project contributed to maintain competence and expertise in the field of reactor safety in the NEA member countries and to promote international co-operation between its member countries.

3. Test configuration, test procedure and test results

This section describes the standard configuration and basic instrumentation of the test facility, the specific configurations and additional instrumentation of each test series, and the test procedures and results specific to each test series.

3.1. Test facility general overview

3.1.1. Two-vessel facility THAI$^+$

The two-vessel facility consists of the original THAI test vessel (TTV), to which a smaller vessel, designated as parallel attachable drum (PAD), is interconnected by a lower and an upper DN500 connection pipe, Figure 3.1. The arrangement of the two-vessel system within the THAI building is depicted in Figure 3.2.

The total gas volume of the facility amounts to about 80 m³. The specifics of the two vessels are described below and more details of the THAI$^+$-facility are provided in the respective Technical Report (Freitag et al., 2016).

The THAI building includes a restricted area in accordance with the respective radiological protection regulations for tests for which a radioactive iodine tracer I-123 is used.

3.1.2. THAI test vessel

The THAI vessel (TTV) is 9.2 m high, has a volume of 60 m³, an inner diameter of 3.2 m, and a sump compartment of 1.7 m³ with an inner diameter of 1.4 m. The vessel is manufactured from austenitic steel 1.4571 (DIN EN 10088-3 X6CrNiMoTi17-12-2 ≈ AISI/SAE 316Ti) with complete thermal insulation. The cylindrical part of the vessel walls is a double walled steel structure with 22 mm inner wall thickness, a 16.5 mm thermal oil gap and 6 mm outer wall thickness and is subdivided in three vertical sections that can be heated or cooled separately. Heating of a section by means of thermal oil is possible up to 160 °C. The (static) maximum overpressure is 14 bar at 180 °C (design value). Complete or partial removable internal steel structures allow the performance of multi-compartment tests or the installation of specific hardware for testing, e.g. PARs, elevated water pools.

Comprehensive process equipment is available e.g. for steam supply (up to 37 g/s at 170°C, 8 bar), compressed air, injection gases like H_2, N_2, He, water/solution spray injection, aerosol generation and injection, and the injection of I_2 (both as gas and liquid) labelled with radiotracer I-123, including the respective equipment for volume flow control and measurement.

3.1.3. PAD test vessel

The PAD has a similar design and the same design specifications as the THAI vessel, but is smaller in volume (V = 18 m³) and inner diameter (ID = 1.6 m), and is slightly higher (H = 9.7 m). The auxiliary and supply systems of the PAD correspond to that of the TTV. The PAD is instrumented like the TTV, but with a smaller number of sensors.

Upper and lower pipe segments (inner diameter 0.5 m) with the same design specifications as the TTV and PAD connect the two vessels.

3.1.4. Instrumentation

For the tests described in this report, comprehensive instrumentation for thermal hydraulics, iodine, aerosol and gases is installed. The standard instrumentation encompasses thermal hydraulic and gas composition instrumentation. It is supplemented by special instrumentation depending on the specific test designs and test objectives.

Feed mass flow measurements

Steam mass flow as well as compressed air mass flow is measured by a float-type gauge (Rotameter).

The mass flow of the gases hydrogen, helium, nitrogen and oxygen (taken from gas bottles) is measured by float-type gauges. For test data evaluation, the integral of the gas mass flow measured with this device is compared with the injected gas mass determined from the start and the end pressure of the gas bottles and compared with the pressure increase in the vessels.

Gas concentration measurement

Up to 25 gas sampling lines continuously take gas samples from the vessel's atmosphere at different locations. The sampled gas is fed to a 25-channel gas concentration analyser system that determines the hydrogen or helium concentration in dry air. In case of experiments with steam, steam is removed by coolers and condensate traps upstream of the analysers. Up to six of the 25 lines for hydrogen/helium concentration measurement are additionally equipped with oxygen sensors. Concentration of hydrogen/helium and oxygen is then determined in dry air. For those experiments for which the steam in the vessel's atmosphere was at saturation state, the real ("wet") concentrations of hydrogen/helium and oxygen in the vessel atmosphere could be determined by use of the steam table for the partial pressure of steam at the temperature measured in the vessel. Otherwise relative humidity measurements are used in the vessels to determine the partial pressure of steam.

Temperature measurement ("slow thermocouples")

Up to 150 calibrated 1.5-mm thermocouples are installed in the TTV and PAD for temperature measurement in the vessel atmosphere with an accuracy of ± 0.3 K for a temperature range 0 °C to 130 °C.

In addition, another 300 thermocouples are installed to measure the wall temperatures of the TTV and PAD.

Temperature measurement ("fast thermocouples")

To monitor the PAR catalyst temperature, flame front propagation and flame temperature during hydrogen combustion, "fast" sheathed thermocouples (outer diameter 0.5 mm) are used. As the arrival of the flame front at the individual thermocouple causes a steep temperature signal rise, the time points of flame front arrival can be determined with an uncertainty smaller than 0.01 s.

Pressure measurement ("slow")

The initial vessel pressure and the pressure increase due to gas injections or gas atmosphere heating are determined by four pressure transmitters and a digital high-precision manometer. The measurements with pressure transmitters are cross-checked with a high-precision manometer (accuracy ± 10 mbar). Also recorded is the absolute atmospheric pressure with a barometer inside the experimental hall.

Pressure measurement ("fast")

The transient of the deflagration is measured with fast piezoresistive pressure transmitters (Keller PAA-M5 HB), using a sampling rate of 1 kHz. The signals of these transducers show a slight temperature influence and therefore are referenced to the "slow" transducer with respect to zero-point deviation and identical pressure decrease after the deflagration event.

Flow velocity measurement

Flow rate at PAR inlet

In order to determine the H_2 recombination rate of a PAR, the H_2 concentration at the PAR inlet, at the PAR outlet and the volume flow through the PAR are to be measured. The latter is achieved by a turbine flow metre ("vane wheel") installed in the inlet flow channel. The vane wheel transducer applied has a lower threshold value for start-stop of vane wheel rotation of approx. 0.25 m/s and a measuring accuracy of ± 0.1 m/s.

METUSA

A unique measurement device (minimal encroaching turnable stream-wise anemometers: METUSA) is installed in the upper connection pipe that makes it possible to determine the volumetric flow being exchanged between the two vessels. It consists of two rotatable flanges that envelope an 885 mm long DN 500 pipe section into which six vane wheels are installed. Each of the 30 mm ∅ vane wheels is installed at a different pipe radius between the centerline and pipe wall. Additionally, all the vane wheels have been installed at different angles and axially over a distance of 100 mm in order to minimise the flow disturbance. By turning the pipe section by 360°, each of the vane wheels run along a circular path. The summation of the six circular paths, each being 30 mm thick, makes it possible to accurately calculate the velocity distribution inside the pipe. During hydrogen deflagration tests, the vane wheels were pulled out of the gas space before triggering the ignition in order to protect the vane wheels from being exposed to high temperatures.

3.1.5. ***Aerosol measurements***

To determine aerosol concentration and particle size distribution, different methods have been established.

Integrating filter (WH-24 and WH-28)

A metal fibre filter is installed in the PAD exhaust line to integrally collect all salt/CsI particles leaving the PAD vessel. Five filter cartridges are operated in consecutive manner during the twelve measurement phases of test WH-24, and during thirteen phases in test WH-28, respectively. When a measurement phase is finished, the particular filter cartridge is leached two times into 5 L of decalcified water after dismantling. Leaching liquids are analysed after the test for salt/CsI content.

Bulk filters

Measurement of the aerosol mass concentration is performed with bulk filters. The filters are weighed before and after the experiment. From gas sample volume flow, the sampling time and mass of the retained particles, a mean aerosol concentration can be calculated for the sampling period. In tests with very low aerosol concentration, chemical analysis is used to determine the aerosol loading.

Gas scrubbers (WH-24 and WH-28)

Two gas scrubbers are installed to measure the aerosol concentration in the gas space. Even though the aerosol concentration at the gas scrubbers only gives information about the local concentration, the aerosol concentration is quasi-stationary during the individual periods of constant gas injections into the sump or during the depressurisation phases.

Cascade impactor

Furthermore, low-pressure cascade impactors are available to determine the particle size and the particle size distribution. The impactors separate ten particle size classes. The mass of each particle class collected during the sampling period is determined by weighing or chemical analysis.

3.1.6. ***Iodine measurements***

The measurement of iodine is mainly based upon the use of detectors for iodine labelled with the radiotracer I-123, samples from gas scrubbers and Maypack filters, or online monitoring of deposition coupons.

Scintillation detectors

Three lead-shielded NaI scintillation detectors outside the test vessels are focused to monitor the I-123 radiation inside the vessel. They indicate the evolution of the iodine activity either on iodine deposition coupons (stainless steel or decontamination paint coated) or in the gas phase. Usually, a standard geometry configuration of detector, shielding (focus) and deposition coupons is used and evaluated based upon calibrated geometries. The measurement is quasi-continuous and typically every 30 s a count rate is recorded during transient phases. During less transient phases, i.e. in later stages of Iod-32, the output of a count rate is slowed down as far as every 10 min.

Gas scrubbers

Measurement of gas-borne iodine concentrations is based on the gas scrubber (GS) technique, with up to eight gas scrubbers. To avoid long gas sampling lines often associated with significant iodine losses, these gas scrubbers are installed inside the vessels at various positions. Absorber solution is fed into and removed from the gas scrubbers from outside the test vessel repeatedly during a test, so that concentration evolutions with time can be determined. After sampling (scrubbing) for several minutes at a gas flow rate 0.5–1 l/min, the absorber is recovered, cooled down and measured by I-123 γ-counting and by UV-VIS spectroscopy. Sampling times vary between 2 min and 30 min, with increasing tendency in the course of a test to account for the depletion of gas-borne iodine by deposition onto surfaces and for the short half-live (13.2 h) of I-123.

Maypack filters

Two Maypack filter sampling stations are available to discriminate gas-borne iodine in molecular iodine (I_2), gaseous organic iodide and iodine in aerosol form. Each Maypack device consists in general of one quartz filter to retain aerosols, two filters to retain gaseous I_2, and two charcoal filters (KI-impregnated) to retain organic iodides. This enumeration defines at the same time the flow direction.

Laser absorption system (LASI)

An additional iodine measurement is performed by iodine specific light absorption, which provides a continuous, in-line and non-intrusive measurement of gas-borne iodine. The 532 nm wavelength laser is emitted by a laser diode located outside of the PAD. The beam is mirrored so that it passes the vessel's diameter four times, resulting in a total optical pathway of 12.6 m. The light absorption at 532 nm is sensitive to molecular iodine (I_2), with minimum cross-sensitivity to the remaining gas mixture, which consists predominantly of N_2, O_2, H_2O and argon.

3.2. Hydrogen deflagration (HD) tests

The objectives of the hydrogen deflagration test series HD-40 to HD-45 are to provide more knowledge and experimental data on the influence of convective flows on the flame propagation of hydrogen combustion and the relevance of scale for flame acceleration effects as a function of the hydrogen concentration. Furthermore, tests should address the effects of hydrogen deflagrations in a two-vessel configuration including stratifications of gas concentration and/or gas temperature. These data are required for model development and code validation purposes taking into account "multi-compartment effects".

To achieve these goals, appropriate hydrogen deflagration tests are performed in the two-vessel THAI$^+$ test facility. In large geometries, deflagrations may proceed faster due to, for example, increased turbulence generation and therefore may produce higher loads for the vessel and its internals.

Details of test series HD-40 to HD-45 are provided in the respective Technical Report (Freitag et al., 2019).

3.2.1. Test configuration

The test configuration for tests HD-40 to HD-45 with the gas injection positions, the internal blower and the igniter positions is shown in Figure 3.3.

The blower was operated to establish a (low-velocity) circulating flow within the TTV and the PAD prior to ignition in forward direction, i.e. gas is sucked from the PAD vessel and blown into the sump compartment and consequently through the lower connecting pipe into the TTV.

Remotely controlled arc igniters are installed in the sump compartment at an elevation of H = 0.5 m and close to the vessel head at H = 9.1 m of the TTV. In all tests only one igniter (either top or bottom) is operated. The integral energy delivered during the igniter operation time of 1s is about 10 J.

3.2.2. Test procedure

Table 3.1 summarises the specified initial test conditions for the tests HD-40 to HD-45. All tests were performed at 1.5 bar initial pressure. Steam, temperature and hydrogen concentration gradients were established in the two-vessel configuration for tests HD-40 to HD-42 under similar conditions as in tests HD-26 to HD-28, performed in the TTV alone in the framework of the NEA THAI project (NEA, 2010). Tests HD-43 to HD-45 were performed under similar initial conditions as HD-36, which was performed in the THAI$^+$ test facility in the framework of the German national THAI program (Freitag et al., 2017a), but without the large blower, i.e. without initially superimposed gas convection. Prior to ignition, the blower was started for tests HD-43, HD-44 and HD-45 to produce an initial flow in the vessels and in the interconnecting pipes. The mixture was ignited at the TTV

sump compartment in all tests except HD-45 where the mixture was ignited at the top of the TTV. One additional pre-test was performed during which the influence of the blower on the flame propagation was quantified without operation of the blower. The test was performed with ignition at the bottom of the TTV, similarly to test HD-36.

Table 3.1. Test conditions as specified and measured for the HD test series

Test ID	Test Parameter					Objectives
	c_{H2} [vol.-%]	c_{st} [vol.-%]	Temp. [°C]	Initial gas flow	Igniter	
HD-40 (spec)	12 top 6 bottom	47 top 3 bottom	90 top 30 bottom	none	TTV bottom	Stratified conditions in 2-vessel system Potential jet ignition effect in positive H_2-concentration gradient Effect of stratification in 2-room compartment on flame propagation Comparison to HD-27 (TTV only) and HD-38
HD-40 (meas)	11.9 top 6.0 bottom	45 top 2 bottom	89 top 34 bottom	none	TTV bottom	
HD-41 (spec)	6 top 12 bottom	47 top 3 bottom	90 top 30 bottom	none	TTV bottom	Effect of negative H_2-concentration gradient in 2-room compartment on flame propagation Comparison to HD-28 (TTV only) and HD-40 Variation of jet ignition effect, interaction of flame fronts
HD-41 (meas)	6.2 top 11.4 bottom	44 top 4 bottom	87 top 34 bottom	none	TTV bottom	
HD-42 (spec)	10 top 10 bottom	47 top 3 bottom	90 top 30 bottom	none	TTV bottom	Potential jet ignition effect in homogenous H_2-concentration Effect of stratification in 2-room compartment on flame propagation Comparison to HD-26 (TTV only), HD-40, and HD-41
HD-42 (meas)	10.0 top 9.5 bottom	45 top 3 bottom	89 top 32 bottom	none	TTV bottom	
HD-43 (spec)	10	25	90	low	TTV bottom	Influence of initial convection in 2-room facility; comparison to HD-22 (TTV only), HD-36
HD-43 (meas)	10	26.0	88.8	0.61 m^3/s	TTV bottom	
HD-44 (spec)	10	25	90	high	TTV bottom	Influence of high initial convection in 2-room facility; comparison to HD-36 and HD-43
HD-44 (meas)	10.2	25	89	1.2 m^3/s	TTV bottom	
HD-45 (spec)	10	25	90	high	TTV top	Influence of high initial convection in 2-room facility; comparison to HD-36 and HD-43 Influence of igniter position HD-44
HD-45 (meas)	10	25.3	89.9	1.2 m^3/s	TTV top	
Pre-test (meas.)	9.95	25.3	88.5	none	TTV bottom	Evaluation of influence of blower Comparison to HD-36 (TTV bottom ignition)

The test procedure for the HD test series consisted of a preconditioning phase, during which the initial conditions were established, followed by the main test phase. Both vessels were dried up and the remaining condensate from previous tests was removed before the tests. To achieve the desired initial thermal hydraulic conditions, the vessel walls were heated to the desired target temperatures. Steam, air and hydrogen injections were performed according to the pre-calculated amounts to generate the desired mixture at the specified temperature and pressure conditions in the vessels.

The main test phase started with the triggering of the igniter at time t = 0 s.

3.2.3. Test results

Deflagration pressure increase behaviour of the 2-vessel system

Slightly lower peak pressures were observed for tests in the 2-vessel THAI$^+$ geometry than for tests in the single vessel (TTV only) with the same initial conditions, Figure 3.4. This applies for well-mixed tests (compare HD-36 and HD-22, Figure 3.4) as well as for tests with a positive H_2-concentration gradient. This finding can be attributed to higher heat transfer in the two-vessel geometry due to a higher surface-to-volume ratio, namely 2.2 for the two-vessel geometry, and 1.67 for the single vessel (Freitag et al., 2017a).

The pressure increase gradient did not differ markedly for the single vessel and the two-vessel configuration. However, pressure increase behaviour was markedly influenced by the operation of the blower, which produces a significantly steeper pressure increase.

All peak pressures remained clearly below the AICC pressures.

Jet ignition effect

Jet ignition is characterised by a three-step process:

1. Flame propagation in the ignition compartment: Due to volume expansion, unburnt mixture is displaced into the downstream compartment. Downstream of the interconnecting opening, the jet produces high turbulence within the downstream compartment.

2. Ignition of the downstream compartment: Once the jet passing the interconnecting opening turns into a flame jet, the inventory of the downstream compartment is ignited instantaneously and the subsequent extremely strong pressure increase might not be relieved by openings further downstream.

3. Post combustion in the ignition compartment: The overpressure in the downstream compartment produces a backflow into the ignition compartment, thereby increasing turbulence, which intensifies the combustion of the residual H_2, producing a steep pressure increase also in the ignition compartment.

Step 2 requires only a few milliseconds, as has been observed also for a relatively large downstream compartment of 80 m³ with 11 vol.-% H_2 in both ignition and downstream compartments, 25 vol.-% steam in the ignition compartment, and 35 vol.-% steam in the downstream compartment (Kanzleiter, T., 1992).

Such a pronounced jet effect was not observed for the present test series. The reason may be as follows: In tests performed by Kanzleiter (Kanzleiter, T., 1992) and other experimenters, the downstream compartment with relief opening remained unpressurised during step 1. Hence, gas transport into this compartment was restricted only by the interconnecting opening, whereas in the present tests both compartments where pressurised at the same time, inhibiting the gas transport into the downstream compartment. During combustion, no pressure difference between the two vessels was observed, i.e. the two-vessel geometry behaved in this respect like a single vessel. This applies also for test HD-45 with the ignition position at the top of the TTV. This ignition position was regarded to be most favourable for a jet ignition effect.

Flame front propagation

Flame front propagation in the TTV, the PAD and the upper connection pipe is depicted as time/travelled distance-function for well-mixed tests in Figure 3.5. For tests HD-40 to HD-42 with H_2, with steam and temperature stratification, an exact determination of a flame

front is not possible due to pronounced flame instabilities and erratic flame propagation. The fast flame travel was remarkable in the PAD for the tests with an ignition location at the TTV's bottom. The reason is the flame acceleration in the lower connection pipe, which creates additional turbulence in the yet unburnt mixture in the lower part of the PAD.

For test HD-36 (same initial conditions as test HD-43, but without initial flow) an extremely fast downward travelling flame was observed inside the upper half of the PAD, which can be regarded as jet ignition.

The apparent negative elapsed time in the upper part of the TTV, Figure 3.5, can be explained by the fact that the elevation of 11 m represents the centreline of the upper connection pipe, in which for tests HD-43 and HD-44 the flame travelled from the PAD to the TTV. For test HD-45, with ignition located at the TTV's top, the flame travelled much faster within the upper connection pipe to an elevation of 11 m than downward in the TTV.

Influence of initial flow on peak pressure

The different initial flow conditions established for the premixed tests were as follows:

- HD-36: no initial flow
- HD-43: = 0.61 m³/s
- HD-44: = 1.2 m³/s
- HD-45: = 1.2 m³/s but with ignition location at the TTV top

The evolution of peak pressures for these tests is depicted in Figure 3.6. Since these tests had slightly different initial H_2-concentrations, the peak pressures were extrapolated to a H_2 concentration of 10.2 vol.-% (HD-44) using the slope of the AICC for an initial pressure of 1.5 bar and an initial steam content of 25 vol.-%. For an H_2-concentration of 10.2 vol.-%, an initial volume flow increases peak pressures linearly if ignition is triggered at the TTV vessel's bottom. For ignition at the TTV's top, a slightly smaller peak pressure is observed, Figure 3.6.

3.3. Hydrogen recombiner (HR) tests

Test results on PAR behaviour have been acquired so far by exposing the PAR to initially stagnating flow conditions. Further experimental investigations that address the influence of containment typical flow conditions on the performance of PARs were considered to be of high relevance for the development and validation of severe accident analysis codes.

In the test series HR-46 – HR-50, the onset and performance of two different commercial PAR units under counter-current flow were investigated. In particular, the tests investigated whether the exposed flow influences the internal PAR behaviour, e.g. its self-induced chimney flow and the recombination efficiency of the catalytic materials.

Details of the test series HR-46 – HR-50 are provided in the respective Technical Report (Freitag et al., 2017a).

3.3.1. Test configuration

The THAI$^+$ configuration consist of the THAI test vessel (TTV) and the smaller parallel attachable drum (PAD), which are connected by two pipe segments of DN 500, Figure 3.1. For tests HR-46 to HR-50, all standard internals (inner cylinder and four lateral condensate trays) were removed from the TTV except all condensate gutters, which collect wall condensate in both vessels.

Further details about the THAI$^+$ test facility and the instrumentation are given in section 3.1. Added to the basic configuration were the following components:

Large axial blower

To produce an initial flow inside the vessels and the interconnecting pipes, a large axial blower was installed for tests HR-46 to HR-49 atop of the TTV sump compartment, Figure 3.7. During all the tests of the series, the blower was operated in reverse direction, hence gas was sucked from the TTV sump compartment and accelerated into upward direction. By this, either a counter-current or co-current flow could be superimposed on the natural convective flow produced by the PAR. No blower was installed for test HR-50.

Passive autocatalytic recombiners

For the tests, PAR units provided by AREVA (now Framatome GmbH) and NIS Ingenieurgesellschaft mbH were used.

The tests HR-46 and HR-47 were conducted with a 1/8 module NIS PAR, Figure 3.7 and Figure 3.8. The catalyst arrangement consists of 11 perforated stainless steel cartridges filled with palladium-coated porous ceramic pellets with a diameter of 4-6 mm. Due to their porosity, the pellets have a very large inner surface that favours catalyst reaction.

In tests HR-48 – HR-50, an AREVA PAR (model FR-380) was installed, Figure 3. The capacity of the PAR unit was scaled down to match the size of the test facility by reducing the number of catalytic foils to approximately 50% of the original number, and by inserting a vertical partition wall to reduce the active PAR flow cross section accordingly. In the present PAR unit, 19 stainless steel foils coated with porous platinum catalyst were arranged with 10 mm spacing in the lower part of the PAR housing. In all tests, only one PAR unit (either NIS or AREVA) was installed inside the PAD.

3.3.2. Test procedure

Table 3.2 summarises the specified and measured initial conditions of tests HR-46 to HR-50 performed in the THAI$^+$ facility. The initial thermal hydraulic conditions of tests HR-46 to HR-48 and HR-50 were set identically to the conditions of tests HR-7 and HR-8, which were performed in the TTV test facility during the OECD-NEA THAI project (Kanzleiter, T., 2009), and of tests HR-43 to HR-45, performed in the THAI$^+$ facility (Freitag et al., 2017a). The reference test for HR-49 is HR-12, which was performed in identical thermal hydraulic conditions as HR-49 but using the TTV vessel only during the NEA THAI project (NEA, 2010). Tests of the current series investigated the effect of counter-current flow on the NIS PAR (HR-46) and the effect of the chimney height on the NIS PAR start-up and performance (HR-47). The strength of the counter-current flow was increased in HR-48 and HR-49 as compared to test HR-43, whereas for HR-49 steam content and pressure were also increased. In test HR-50, the AREVA PAR was exposed to natural convection inside the THAI$^+$ configuration.

Table 3.2. Test conditions as specified and as measured for the HR test series

Test #		P_0 [bar]	T_0 [°C]	c_{Steam} [vol.%]	PAR unit	Flow velocity in vicinity of PAR [m/s]	Flow velocity at PAR inlet [m/s]	Objective
HR-46	specified	1.5	75	25	NIS	≈ 0.5 (blower)		Effect of counter-current flow
	measured	1.5	77.2	27.2		0.87	0.44	
HR-47	specified	1.5	75	25	NIS	≈ 0.5 (blower)		Chimney effect in counter-current flow
	measured	1.5	77.8	27.8		0.85	0.41	
HR-48	specified	1.5	75	25	AREVA	≈ 1.0 (blower)		Strength of counter-current flow
	measured	1.5	77.6	26.9		*	0.34	
HR-49	specified	3.0	117	60	AREVA	≈ 1.0 (blower)		Pressure and temperature; counter-current flow
	measured	3.0	119	61.6		1.45	0.32	
HR-50	specified	1.5	75	25	AREVA	natural convection by wall heating/ cooling		PAR exposed to natural convection
	measured	1.51	100.8	17.1			-	

Note: * vane wheel above PAR failed during the test

The test procedure for the HR test series consisted of a preconditioning phase followed by the main test phase. The desired thermal hydraulic conditions and the steam contents as depicted in Table 3.2 were established in the preconditioning phase. The main test phase started with the release of hydrogen into the vessel. Time t = 0 s corresponds to the start time of the first hydrogen injection to reach the target concentration level.

3.3.3. Test results

The comparison of the test results of HR-46 and HR-47 and of the previous HR tests using the NIS PAR under similar thermodynamic boundary conditions (Kanzleiter, T., 2009), reveals that the first onset of hydrogen recombination is much faster under conditions of counter-current flow in the THAI$^+$-facility. However, the recombination rate is significantly reduced as long as the hydrogen concentration remains below about 2-3 vol.-% for these two tests due to an initially stable downward flow and later oscillations of the flow direction inside the recombiner. As soon as the hydrogen concentration at the PAR inlet exceeds about 3-5 vol.-%, a stable upward gas flow inside the recombiner was established and the recombination rate of HR-46 matched the test results of HR-14, whereas the recombination rate of HR-47 remained reduced. Both during the first and second hydrogen injection phase of test HR-47, flow oscillations were observed for relatively high H_2-concentrations.

In Figure 3.10, the hydrogen depletion efficiency of HR-14, HR-15, HR-46 and HR-47 is depicted as a function of the hydrogen concentration at PAR inlet. For hydrogen concentrations above a certain value, the hydrogen depletion efficiency of HR-46 matches the results of HR-14 and HR-15 with values between 50 and 60%. Below a certain concentration, lower efficiencies are recorded for HR-46 due to the oscillations of flow direction. For test HR-47 with reduced chimney height, the efficiency is increased by about 10% due to reduced internal gas velocity, which in turn increases the residence time of the hydrogen at the catalytic cartridges. However, the reduced self-induced buoyancy makes

the PAR in HR-47 more susceptible to the external counter-current flow, which induces oscillations already at low hydrogen concentrations.

Apart from the delayed PAR start-up behaviour during the second hydrogen injection sequence in test HR-47, no measurable impact on the catalyst temperature could be identified by exposing the PAR to counter-current flow conditions.

During tests HR-46 and HR-47, glowing particles were detected inside the PAD and TTV. Owing to their very low density, these "glow worms" remained airborne for an extended period of time and were transported within the large convective loop that was driven by the blower. Even though no dedicated measurements were installed to quantify the exact time of the first appearance of these glowing particles, they could be traced visually as long as the hydrogen content inside the THAI+ system was above 4 vol.-%. Below this concentration their frequency of appearance reduced significantly.

In Figure 3.11 the start-up of the AREVA PAR under counter-current flow conditions (tests HR-43 and HR-48) is compared to tests HR-7 and HR-8 with quiescent conditions and similar thermodynamic initial conditions, Figure 3.11. The onset of recombination during test HR-43 with reduced blower frequency was detected at a certain (relatively low) H_2-concentration and at slightly higher concentration during HR-48 with maximum blower frequency. Under quiescent flow conditions, in tests HR-7 and HR-8 the first indication of PAR operation was detected at noticeably higher H_2 concentrations.

The impact of the counter-current flow conditions on the depletion efficiency for hydrogen concentrations above a certain value is also small, Figure 3.12; i.e. tests HR-43 and HR-48 indicate similar efficiencies of 60 – 70% as HR-7 and HR-8. For decreasing hydrogen concentration, the efficiency of tests HR-7 and HR-8 increases to 80% and 90%, respectively, while the efficiency for test HR-48 decreases to 50%. This decrease is caused by PAR internal flow oscillations due to competing downward-directed flow from the blower and self-induced upward directed buoyancy driven flow. Though this reduces the performance of the recombiner, the overall recombination rate under such low hydrogen concentration is generally small; hence, the reduced efficiency under these conditions impacts the overall hydrogen depletion only marginally.

3.4. Tests with aerosol release from a pool (WH-tests)

Tests WH-24 and WH-28 aimed at quantifying the re-entrainment of soluble fission products (CsI-aerosol) from water pools at elevated temperatures. In test WH-24, de-mineralised water was used initially, while in test WH-28 a surfactant was added to reduce the surface tension of water.

The focus of the investigations was on the re-entrainment of aerosols relative to the initial amount dissolved in water and on water pool hydrodynamics (e.g. bubble dynamics) under realistic containment conditions. These investigations shall contribute to the validation and further development of dedicated empirical or semi-mechanistic models of advanced LP and CFD codes used for reactor applications by providing experimental data.

Details of the tests are provided in the respective Technical Reports (Freitag et al., 2017b), (Freitag et al., 2018).

3.4.1. Test configuration

The configuration of tests WH-24 and WH-28 consists mainly of the smaller vessel of the THAI$^+$ facility, namely the parallel attachable drum (PAD), Figure 3.13. The THAI test vessel (TTV) is used as a reservoir for hot gases released from the PAD vessel. The benefit of using the PAD as compared to the TTV is a smaller particle dilution inside the gas space

above the water pool, which improves detection limits of particle measurements by filters, impactors and gas scrubbers.

Additional process components

Added to the basic configuration (see section 3.1) were the following components:

Downcomer pipe

A DN 100 steel pipe (105 mm ID, 4.6 mm wall thickness) is installed in the PAD vertical axis as a downcomer,

Air injection

Air is either injected into the vessel as purging air to allow for superheated conditions inside the vessel and or into the sump via the downcomer pipe for bubble generation.

Water injection

Cold decalcified water is injected into the PAD sump at bottom centre. Water is injected at the beginning of the test, and if necessary, later in between phases to maintain the water level in the vessel.

Salt (CsI) dosing

A large vessel for salt injection at the beginning and a smaller vessel of 8 L volume for re-injection during the test are installed. High concentrated salt is injected into the PAD sump via a pipe. Salt is injected via this dosing vessel if necessary, in between test phases to compensate for concentration reduction by condensing steam or loss through the spill-over lines.

Gas exhaust line

The gas inside PAD is relieved at its top into the TTV.

Spill-over lines

Two spill-over lines are installed inside the PAD sump compartment, both connected to filling funnels of 60 mm diameter. The spill-over lines are connected to the two condensate collectors outside of the PAD vessel to measure the water volume that was removed from the PAD sump.

Additional instrumentation

Added to the basic instrumentation (see section 3.1.4) were the following components:

Sump salt concentration

The sump recirculation line is connected to an online electrical conductivity sensor. It is used to measure the salt concentration inside the pool water during the test using a predetermined calibration.

Bubble measurements

Gas bubble measurements are based on a high-speed camera and image processing software. The PAD vessel sump was equipped with optical accesses at H = 0.65 m and H = 2.1 m. A high-speed camera (Photron FastCam SA 1.1) that records 1 000 frames per

second was alternately placed at these optical accesses. The focusing depth was approximately 10 mm. This arrangement makes it possible to track bubble dynamics of the uprising air, steam, or steam/air bubbles.

3.4.2. Test procedure

Tests WH-24 and WH-28 were divided into individual phases (12 for WH-24 and 13 for WH-28) that are grouped into three phenomenological categories:

a) Particle re-entrainment from a heated pool by injection of air and steam/air mixtures

b) Particle re-entrainment from boiling pool by injection of steam and steam/air mixtures

c) Particle re-entrainment from flashing pool induced by depressurisation

In Table 3.3, the individual test phases are specified. Details of the test procedure discussed in the following refer to test WH-28; those of test WH-24 are essentially the same. Test phases a1) to b4) are performed at stationary pressure conditions, i.e. 2.5 bar, using the regulation valve that is installed in the upper connecting pipe between PAD and TTV. To dry out the salt loaded water droplets that will be released from the water pool, a sufficient superheating of the vessel atmosphere is required to obtain aerosol particles. This superheating is ensured by vessel wall heating to approximately 140 °C and by the injection of pre-heated purge air above the water surface. The water volume inside the sump is regulated by using the spill-over lines before each test phase.

Pool flashing was induced by depressurisation. The depressurisation rates of phases c1) to c3) refer to accident conditions during a filtered containment venting operation of a German SWR72 type BWR or Japanese BWR, whereas c4) is envisaged at significantly lower pressure reduction being typical for PWR with a large containment volume. The specified initial test conditions and the envisaged flow rates during the subcooled pool phases (a1 to a5), the boiling pool phases (b1 to b4) and the depressurisation phases (c1 to c4) are listed in Table 3.3.

Table 3.3. Specified test conditions for the phases of test WH-28

Test phase	Air injection flow rate (kg/h)	Steam injection flow rate (kg/h)	Water temperature (°C)	Purge air flow rate (kg/h)	Depressurisation rate
a1)	80	-	46	0	
a2)	80	-	60	0	
a3)	19	70	60	145	
a4)	19	70	90	145	
a5)	19	70	120	145	
b1)		70	boiling	145	
b2)		210	boiling	145	
b3)		350	boiling	145	
b4)	19	210	boiling	145	
c1)	-	-		-	BWR type 1 bar/5 min
c2)	-	-		-	BWR type 3 bar/5 min
c3)	-	-		-	BWR type 1 bar/ 15 min
c4)	-	-		-	PWR type 0.1 bar/30 min

3.4.3. Test results

WH-24

In the WH-24 test, the sump of the vessel was filled with about 4.6 m^3 of water in which 10 g/L caesium iodide (CsI) was dissolved as a representative fission product. The aerosol re-entrainment was quantified based on the concentrations of CsI particles released from the sump.

The bubble measurements performed using decalcified water without additional CsI to protect the high intensity light sources from high halide content inside the water pool provided useful insights about the phenomenology of the gas release from the downcomer. The gas release from the downcomer exhibits two kinds of appearance; a quasi-homogenous gas release as shown in test phases a3), a4) and b1) is characterised by low injection rates of non-condensed gases, and a pulsed gas release as shown in phases a1), a2), a5), b2), b3) and b4) Figure, 3.14 and Figure 3.15. With respect to bubble dynamics, some differences, such as primary bubble formation frequency and maximum ascending height before break-up into globules, and bubble size at water surface are observed between present results and the literature e.g. EPRI tests (Paul et al., 1991). As an example, a cascaded reduction of bubble sizes from initially large structures was not recorded in the present study and a complete break-up of the primary bubble occurred within 3- 4 times the primary bubble diameter. The most significant difference between the actual THAI tests and the EPRI test (Paul et al., 1991) is the temperature of the water pool and the pressure above the water surface – EPRI tests being performed at ambient pressure using cold water (20°C).

In all test phases, particle size distribution measurements with cascade impactors were performed. Generally, very small particles were measured using the impactors, see Figure 3.16. Overall, the particle sizes were very similar, which can be explained by the fact that all measurements were performed within the deposition-controlled region. Large water droplets that might have been generated in the transition region under high superficial velocities did not exceed a height of 2 m above the water surface which was found to be the transition region between momentum controlled and deposition-controlled region according to Kataoka and Ishii (1984).

Entrainment rates between $E = 5 \cdot 10^{-6}$ and $E = 8 \cdot 10^{-5}$ were determined based on different measurement techniques during test WH-24. Even though a large scatter was observed in the measurements in each of the test phases, two main trends can be identified. The entrainment increases for increasing superficial velocities as long as the two-phase flow can be attributed to the bubble flow regime and the entrainment rate is constant, or even slightly decreasing, within the transition regime and the churn turbulent flow regime while increasing the superficial velocities further. This finding is supported by Figure 3.17, which indicates that the average bubble diameter increases for increasing injection Weber number. Therefore, hence the relative frequency of bursting bubbles reduces for increasing gas injection rates.

In this context it needs to be mentioned that WH-24 was the only test where gaseous injection into the pool was carried out by means of a downcomer pipe. Most of the other investigations used a heating coil installed into the sump to generate steam bubbles. The entrainment rate itself can be influenced by additional parameters apart from the superficial velocity, e.g. by the atmospheric pressure (von Rohr, 2000).

WH-28

Direct measurement of the bubble column by high-speed digital imaging was not performed in test WH-28 due to a high opaqueness created by adding the surfactant and antifoaming liquid. Therefore, a separate lab test series was conducted to evaluate the influence of the surfactant on the bubble column behaviour. Measurement of the bubble column width was used to approximate the superficial velocity based on the area through which the gas bubbles break through the pool surface. Test WH-28 covered a similar range of superficial velocities as test WH-24, ranging from 0.01 to 0.12 m/s.

Effect of surfactant on entrainment

The droplet entrainment in test WH-28, using pool water with reduced surface tension, was measured in 13 test phases. Compared to WH-24, the pool water was conditioned with a thermally stable surfactant, which reduced the surface tension to about 25-30 mN/m as compared to 70 mN/m for decalcified water at room temperature.

Entrainment rates between $\mathrm{E} = 3 \cdot 10^{-6}$ and $\mathrm{E} = 3 \cdot 10^{-3}$ were determined based on different measurement techniques during test WH-28, with generally very low values during the flashing phases and very high values during subcooled and boiling phases located in the bubble flow regime.

By comparing the results of tests WH-24 and WH-28, it can be concluded that the entrainment calculated from the aerosol measurements in tests with a surfactant was about one order of magnitude higher compared to the de-mineralised water of test WH-24. Results from different particle measurement techniques that have been used to evaluate the entrainment in tests WH-24 and WH-28 indicate that the absolute entrainment is subject to uncertainty by a factor of 2 – 5.

Effect of surfactant on size of released particles

The addition of the surfactant favoured the release of larger droplets, which in turn might explain the larger entrainment rates, under the assumption that a similar droplet entrainment frequency is given.

The mass median particle diameters during the flashing phases exhibited a similar increase as for the subcooled and boiling phases of tests WH-28 and WH-24. Assuming the absolute entrained mass to scale with MMD^3, an increase of the entrainment by 10 to 30 could be expected. Therefore, it must be concluded that the number of droplets generated when flashing a liquid of reduced surface tension is smaller compared to flashing decalcified water.

3.5. Iodine release from a boiling pool – test Iod-32

The mass transfer of volatile iodine at the gas/water interface is covered in most iodine behaviour codes by the two-film theory, which describes the exchange of volatile iodine in both directions. Mass transfer models for non-boiling conditions are established; however, experimental data on a technical scale to develop or to validate mass transfer models in boiling conditions are sparse. Sump boiling increases both the water motion and the surface area between sump water and gas phase, which will be available for the iodine mass transfer, e.g. by the formation of ascending steam bubbles. Therefore, it was expected that volatile iodine is released much faster in boiling conditions than in non-boiling conditions. The test Iod-32 was aimed at quantifying this effect.

Details of test Iod-32 are provided in the respective Technical Report (Funke et al., 2018)

3.5.1. Test configuration

The configuration of test Iod-32 consists mainly of the smaller vessel of the THAI$^+$ facility, namely the parallel attachable drum (PAD) Figure 3.18. The TTV is used as a reservoir for gases released from the PAD vessel. The benefit of using the PAD compared to the TTV is a smaller dilution of the iodine release from the pool inside the gas space above the water pool, which improves the detection limits of iodine measurements by online sensors and gas scrubbers.

Supply systems and instrumentation correspond to those of test WH-24, see section 3.1.4. Additionally, the following devices were installed:

Iodine injection

The iodine injection consists of a 5 L dosing vessel mounted inside a glove box and a pressure accumulator upstream the dosing vessel. Steel tubes (9 mm inner diameter) connect the pressure accumulator, dosing vessel and PAD vessel. The pressure accumulator is filled with defined amounts of diluted H_2SO_4 for each iodine injection, to support fast and quantitative emptying of the iodine solution from the dosing vessel into the PAD sump water. The dosing vessel contains the I-123-labelled aqueous I_2 solution for each iodine injection.

Spray system

The TTV is connected to the PAD via the exhaust line. To increase the reservoir capacity of the TTV, its pressure is reduced to about 0.5 bar before the iodine injection. A spray system is installed to cool down the atmosphere and to condense steam that is injected from the PAD into the TTV during several test phases. The resulting pressure reduction in the TTV will increase its reservoir capacity with respect to the PAD.

The spray operates by recirculating water from the cold TTV sump. Spray water also covers the walls, efficiently transporting all iodine into the TTV sump by iodine wash-out from atmosphere and by iodine wash-off from surfaces. The iodine inventory in TTV is thus simply monitored by sampling from the recirculated TTV sump.

Online detectors for deposited iodine and gas-borne iodine

Three lead-shielded NaI scintillation detectors outside the test vessel are focused to monitor the I-123 radiation from inside the vessel. They indicate the evolution of the iodine activity either on iodine deposition coupons or in the gas phase. The measurement is quasi-continuous and typically every 30 s the count rate is recorded during transient phases. During less transient phases, i.e. in later stages of Iod-32, the count rate is recorded every 10 min.

3.5.2. Test procedure

The procedure for test Iod-32 consisted of a preconditioning phase followed by the main test phases, as listed below:

- Preconditioning phase to establish initial conditions in the THAI facility
- I_2 release from non-boiling sump (reference phase, pH 3)
- I_2 release from boiling sump at low steam injection rate, pH 3
- I_2 release from boiling sump at high steam injection rate, pH 3
- I_2 release from boiling sump at high steam injection rate, pH~9

The specified initial test conditions are listed in Table 3.4 and Table 3.5 for PAD and TTV, respectively. The desired thermal hydraulic conditions were achieved by heating of the PAD walls and controlled air injections. The pool water temperature was increased using steam injections through the downcomer. The time t = 0 is defined as beginning of the first iodine injection into the PAD sump.

Table 3.4. Specified test conditions in PAD

Test phase	p (bar)	T (°C)	c_{Steam} (vol.-%)	PAD sump
Pre.	2.5	117 (gas) 110 (water)	72 (satur.)	Initial filling deionised water 1028 L, H= 0.25 m inside PAD Conditioning to pH= 3
1	2.5		up to 90	Injection of ~1 g radio-labelled I_2 Activity ~0.5 GBq
2	1.3 bar after depressurisation		up to 90	Injection of ~1 g radio-labelled I_2 Activity ~ 0.5 GBq Steam inj. mass flow rate 5 g/s, injection duration 10 min
3	1.3 bar after depressurisation		up to 90	Steam inj. mass flow rate 20 g/s, injection duration 10 min
4	1.3 bar after depressurisation		up to 90	NaOH injection to reach pH = 9, Steam inj. mass flow rate 20 g/s, injection duration 10 min

Table 3.5. Specified test conditions in TTV

Test phase	P (bar)	T (°C)	c_{Steam} (vol.-%)	TTV sump
Pre.	0.5 (partial vacuum)	20 (gas)	0	Initial filling deionised water 500 L, H = 0.43 m inside TTV Conditioning to pH ~9
1 – 4	Vacuum pump will be switched off and remain off before injection of iodine into PAD, TTV pressure will rise during each injection phase, spray system running			

Iodine injection

The measurement of iodine in Iod-32 was essentially based upon the use of I-123 radiotracer (T1/2 = 13.22 h). An activity amount of 1.11E+9 Bq was delivered for test Iod-32. The I-123 activity was divided into two parts to enable two iodine injections. For each I_2 injection, 4.7 L of I_2 solution in diluted H_2SO_4 (pH 1.4, 0.038 mol/L) was prepared, obtained from dissolving solid I_2 globules. About half of the I-123 activity was added. Samples were taken to quantify the injected amounts of I-123 and I_2.

3.5.3. Test results

The first I_2 injection (0.73 g) started the reference phase, phase 1, and a small, constant gaseous I_2 level of about 1E−7 g/L was observed after a certain time in the PAD gas space, due to I_2 mass transfer at the gas/water interface in non-boiling conditions (see Figure 3.19), though the I_2 in the sump was completely consumed during phase 1. To run the first boiling phase, phase 2, a second I_2 injection (0.73 g) was performed. The sump boiling increased the gaseous I_2 concentration by two orders of magnitude (see Figure 3.19). The online detectors indicated that the initiation of boiling by depressurisation of the PAD was predominantly increasing the I_2 in the PAD atmosphere, and that the quasi-stationary boiling

by steam injection into the sump for 10 min produced a further but slower increase of the gaseous inventory. Taking into account that the gas atmosphere is permanently transferred to the TTV during the steam injection and boiling phase, this slow increase indicates however that still considerable amounts of I_2 are released from the sump to the gas phase.

The results of several sump measurements in the PAD provide a consistent view of the I_2 evolution in the sump during the test. I_2 masses in the PAD sump as obtained from the different chemical analyses agree well with each other, Figure 3.20. The scattering of the data, especially for the iodide electrode data, was within known bands of data uncertainties. After both I_2 injections the aqueous I_2 was depleted at approximately the same rate, which is equivalent to a half-life of 14 minutes, pre-dominantly by I_2 reaction with the immersed steel walls of the PAD sump. The rate was very similar in both test phases and can be averaged to 3 / h. This short half-life was limiting the amount of I_2 release to the gas phase. The I_2 depletion rate is also similar to a down-scaled GRS/COCOSYS design calculation. This I_2 measurement is important for calibration of models of I_2 conversion into iodide at immersed steel surfaces. As there was no more I_2 available in the sump at the end of phase 2, the planned second boiling phase at an increased steam injection rate was skipped.

The boiling at the beginning of the alkaline test phase 3 did not increase the gas-borne iodine in the PAD atmosphere. The volatile iodine in the sump had been consumed already during phase 2 and no release of volatile iodine was expected anyway. Additionally, phase 3 showed that there was no release of non-volatile, droplet-bound iodine.

Compared to the I_2 release from the sump in non-boiling conditions during the reference phase, the I_2 release due to boiling was higher by roughly a factor of 10. This I_2 release factor was limited in Iod-32 by the fast I_2 depletion in the sump water due to the I_2 / steel reaction.

In the gas phase, the first boiling increased the I_2 concentration by a factor of 100. This effect is obviously influenced also by the adsorption/desorption of I_2 onto/from steel walls exposed to the PAD gas atmosphere. The presence of a gaseous stratification just above the sump is also strongly suspected (for geometric and thermal hydraulics reasons). It might have led to (1) an inhomogeneous iodine concentration in the gaseous phase and (2) to an underestimation of the measured iodine gaseous concentration at the equilibrium in non-boiling conditions.

The additional test objective to measure an equivalent I_2 release from the sump during boiling at an increased steam injection rate could not be realised, due to the complete I_2 consumption during the previous test phase.

The overall iodine mass balance at the end of the test was essentially closed (91%), including inventories in the PAD and the TTV.

3.6. Iodine resuspension - test Iod-34

The objective of test Iod-34 was to measure the resuspension of iodine from painted surfaces by hydrogen deflagration, where the (thermally aged) paint was pre-loaded with gaseous iodine in a representative manner. Iodine measurements in the test vessel were performed to determine the rate and efficiency of I_2 deposition on painted surfaces and steel surfaces, to determine the speciation of the released iodine (iodine in aerosol form, molecular iodine, organic iodide), and to monitor the iodine loadings on the surfaces. This requires the use of the I-123 radiotracer technique. Furthermore, paint degradation was to be characterised.

Details of test Iod-34 are provided in the respective Technical Report (Funke et al., 2019).

3.6.1. Test facility

The THAI$^+$ configuration for test Iod-34 consists of the TTV and the smaller parallel attachable drum (PAD) (Figure 3.1). In this configuration, the PAD is only used for storing the iodine-loaded spray water after spraying in the TTV for iodine sampling. Figure 3.21 shows details of the TTV test configuration as used for Iod-34 test.

For a detailed description of the test configuration with basic process equipment and instrumentation, see section 3.1. Additional equipment and instrumentation used for test Iod-34 are described in the following.

3.6.2. Additional process equipment

Painted surfaces

The whole painted surface area of test Iod-34 amounts to 10.65 m², established by painted coupons inside the TTV. The epoxy-type paint was GEHOPON, representative for German containments and a THAI standard. All painted surfaces were artificially pre-aged by thermal treatment for 21.1 h at 160 °C in air atmosphere, which is a THAI standard procedure.

The main part of the painted surface area (93.9%) was provided as 20 square steel sheets, 1.5 mm thick, 500 mm edge length, painted on both sides, and distributed within the TTV.

Two completely painted cylindrical deposition coupons, made of stainless steel were within the TTV for online monitoring of the iodine deposition on paint.

The post-test surface analyses of some of these smaller coupons ("PTA coupons") include SEM/EDX and microscopic analyses performed by Framatome at Erlangen. Additional surface analyses, especially FTIR spectroscopy on some PTA coupons were also performed by IRSN at Cadarache.

Igniter

A remotely controlled arc igniter was installed in the TTV sump compartment at an elevation of H = 0.5 m. The ignition is initiated by delivering an arc sequence of 1 s duration. The integral energy delivered during the igniter operation time of 1 s is 10 J.

Iodine injection

Gaseous iodine is injected into the TTV with pre-heated synthetic air as carrier gas from a 10 L gas bottle. The carrier gas is directed onto a baffle plate in the centre axis. The injection is a THAI standard for I_2 puff release injections.

The injected chemical form is gaseous molecular iodine, I_2, radio-labelled with I-123. To promote a quantitative I_2 injection, the carrier gas flow is usually maintained for 10 minutes.

Spray system

In the TTV, an upwardly oriented spray nozzle is installed at an elevation of H = 8.4 m at the centreline. The spray operates by injecting decalcified water stored in intermediate bulk containers.

3.6.3. Test procedure

The test procedure for the Iod-34 test consisted of a preconditioning phase followed originally by the main test phases, as listed below.

Phase 0. Preconditioning phase to establish the specified initial test conditions in TTV

Phase 1. I2 injection and deposition of I2 onto the painted surfaces (and steel surfaces)

Phase 2. Fresh water spray for removing the iodine from gas phase and steel surfaces

Phase 3. Spray water removal, superheating of vessel atmosphere and H2 injection

Phase 4. Release of iodine from paint due to deflagration

The specified initial test conditions are listed in Table 3.6.

The desired thermal hydraulic conditions were achieved by heating the TTV walls to about 90 °C and by the controlled injections of air, steam, and hydrogen and the respective pressure adjustments. The gas concentration measurement system was switched on and off regularly during the hydrogen injection sequence to reduce sampling losses.

The time t = 0 min was defined as the time of the onset of the I_2 injection. Ignition was triggered at t = 1 200 min.

Table 3.6. Specified test conditions in TTV

Test phase	p bar abs.	T_{Gas} °C	c_{Steam} vol.-%	C_{H2} Vol.-%	Phase description
1	1.35	90	25	none	I_2 injection and depletion
2	Three times spray operation with 1 m³ decalcified water each				Removal of gaseous I_2 and iodine deposits on steel walls
4	1.5	90° C	25	10	H_2 deflagration and iodine resuspension

3.6.4. Test results

Phase 1: I_2 deposition

During the first test phase, the initially injected gaseous I_2 was removed from the gas phase by deposition onto painted and steel surfaces. Within 5 hours, the gaseous I_2 was decreased to a level of less than 1% of the initial injection.

Phase 2: Sprayings

Three sprayings were performed during phase 2. After the end of the three sprayings the gas-borne iodine concentrations were further decreased. About 30% (≙ 0.3 g) of the injected iodine (1 g) not fixed on the painted surfaces was removed, consistently determined from samplings in the TTV and PAD sumps.

A complete wash-down of the iodine loadings from steel surfaces was not clearly evidenced. Thus, uncertainty remains over the actual iodine loading on the steel surfaces of the TTV after the spraying and the iodine distribution between paint and steel surfaces cannot be quantified.

The gas phase iodine concentration just before H_2 deflagration was at a very low level of about 2E-8 g/l, i.e. the gas phase was practically free of iodine. An increase in iodine concentration in the gas phase due to deflagration can thus be measured accurately.

As expected, most of the iodine previously deposited on the painted surfaces remained there after washing, so the paint represents a sufficient iodine source for a sensitive measurement of iodine released to the gas phase during the test phase with H_2 deflagration.

Phases 3 and 4: H_2 deflagration

The H_2 deflagration strongly degraded the painted surfaces, showing blistering, cracks and craters, Figure 3.22.

Consistent with paint degradation, significant aerosol concentration was observed visually. No direct aerosol sampling had been foreseen, and the measurement of the total organic carbon from gas scrubbers and gas sampling tubes turned out not to achieve the necessary sensitivity for aerosol measurement.

Gaseous organic iodide was measured after deflagration at levels representing 50% of the total gas-borne iodine. This is by far the highest organic iodide concentration ever produced in a test with painted surfaces in THAI. The composition of the other 50% of gas-borne iodine cannot be concluded uniquely based upon measurements. The observation of a gas-borne iodine concentration being persistent over 5 hours allows two interpretations of the other 50% iodine fraction, namely (1) iodine in an aerosol form of very small particle diameters, and (2) iodine as molecular iodine, whose deposition back onto the paint is hampered by paint degradation. The H_2 deflagration strongly degraded the painted surfaces, showing a flaky structure in the paint, including blistering, cracks and craters. Degradation was approximately similar over the whole THAI vessel, and was increased at the edges of the painted coupons.

Since the distribution of the primary iodine loading between paint and steel surfaces is uncertain, the iodine release fraction from paint can be estimated to be in the range of 4% to 9% of the primary loading. This assessment is based on the measurement of iodine in the gas phase of the TTV after deflagration with the Maypacks, and on the results of the online monitoring of steel and painted deposition coupons.

The release of iodine from paint in aerosol form due to hydrogen deflagration is a new path for iodine containment codes. The paint degradation probably also changes the conditions and the mechanism for thermal release of volatile organic iodide from paint. As the thermal release of volatile organic iodide from paint is so far modelled in iodine codes using only a simple fractional release rate with an Arrhenius-type temperature dependency, such a model is not necessarily suitable for extrapolating to deflagration-relevant temperatures. Furthermore, surface temperatures instead of gas temperatures probably need to be used for scaling, at least for iodine releases in fast transients like hydrogen deflagrations.

3.7. Aerosol resuspension by hydrogen deflagration - test HD-46

The objective of test HD-46 was to measure the resuspension of aerosols deposited on vertical, horizontal and containment-typical grating surfaces by a hydrogen deflagration with ignition at the bottom of the vessel. Furthermore, the test aimed to investigate the release of gaseous iodine by thermal decomposition of CsI particles due to hydrogen deflagration.

Details of test HD-46 are provided in the respective Technical Report (Freitag et al., 2019).

3.7.1. Test configuration

The test configuration for test HD-46 with the CsI injection position, the grating positions and some of the aerosol instrumentation are shown in Figure 3.23. Though not shown in the figure, four gas scrubbers were used as further aerosol instrumentation.

Six slabs of containment-typical gratings were installed in the vessel at two heights and three different azimuthal angles. The total surface area of these gratings was 1.95 m². About 25% of the total horizontal cross section was occupied by metal bars. In all, 22 deposition coupons representing horizontal (11 coupons) and vertical (11 coupons) surfaces of the vessel were installed.

The spark igniter was located at the bottom of the THAI vessel.

For a detailed description of the test configuration with basic process equipment and instrumentation, see section 3.1.

3.7.2. Test procedure

The test procedure for the HD-46 test included a preconditioning phase followed by the main test phases as listed below:

Phase 0 Preconditioning phase to establish initial conditions in the THAI vessel

Phase 1 CsI injection and deposition onto surface

Phase 2 Pressure relief and recovering of coupons

Phase 3 Establishing specified conditions for the deflagration in the THAI vessel

Phase 4 Measurement of CsI resuspension and I_2 release from CsI due to deflagration-induced high-temperature conditions.

CsI particles were injected into the THAI vessel using a two-fluid nozzle with compressed air as carrier gas. The CsI aerosols deposit by stirred settling onto the vertical and horizontal walls as well as on step gratings, which are commonly used as staircases or raised floors in containments. Deposition coupons were recovered after four days of settling time to quantify the particle distribution among the surfaces, resulting in 7 wt.-% on vertical walls, 6 wt.-% on six typical step gratings and the remaining mass on the lower dished head and the sump compartment of the vessel.

The specified initial test conditions are listed in Table 3.7. The desired thermal hydraulic conditions were achieved by heating the TTV walls and controlling the air, steam and hydrogen injections. The time t = 0 min is defined as the time when the CsI injection started, while time t_{HD} = 0 min is defined as the initiation of the hydrogen deflagration.

Table 3.7. HD-46: Specified test conditions in TTV

Test phase	p bar abs	T_{Gas} °C	c_{Steam} vol.-%	c_{H2} vol.-%	Phase description
1	1.3	90			CsI injection and depletion
4	1.5	90	25	10	H_2 deflagration, CsI resuspension and decomposition

3.7.3. Test results

Hydrogen deflagration

The peak pressure during the deflagration was below five bar. This pressure is almost identical to the reference test HD-22. Measured temperatures exceeded 900 °C in the centreline of the TTV.

Aerosol resuspension

The filter measurements performed during test phase 3, before the deflagration, reveal loadings on the filter paper that are below the detection limit of the measurement system. The aerosol concentrations are therefore considered to be below 0.01 g/m^3. The particle

loadings at all stages of the impactor were below the detection limit as well. This makes it possible to conclude that the aerosol concentration inside the vessel was negligible before the hydrogen deflagration. A total of 242 g CsI was injected during phase 1 into the THAI vessel.

The first two impactor measurements after the hydrogen deflagration, starting at t_{HD} = 5 and t_{HD} = 50 min, exhibit a pronounced bimodal distribution. About 8% of the mass collected on the impaction stages belongs to the very fine particles and about 92% of the mass corresponds to the larger MMD. The size of the very fine particles remains similar for the next impactor measurement, starting at t_{HD} = 50 min, but the larger MMD increases, indicating particle growth. The particle mass of the fine particles reduced to about 3% relative to the totally collected mass.

With respect to the thermal decomposition of CsI in test HD-46, the mass ratio of gaseous iodine relative to the gas-borne CsI, $c_{I,gas}/c_{CsI}$, was about 1% for the first GS measurement and decayed rapidly due to the depletion of gaseous I_2. This finding of test HD-46 corresponds roughly to a conversion factor of 2%. The thermal decomposition of CsI by a hydrogen combustion has been investigated by various experimenters (Nelson, et al., 1985), (Kupferschmidt, et al., 1992), (Brown et al., 1990), (Schmitt, al., 1993), (Gupta et al., 2009), (Deschamps and Sabroux, 2003). Conversion factors between 1.4% and 50% were reported by the experimenters. However, initial test conditions (pressure, temperature, steam content), test facilities (vessels, burners, PAR), and test procedures (particle generation, particle injection, particle size distribution, gas composition prior to deflagration, standing flames, particle flow through PAR) were so different that a direct comparison is not possible.

Figure 3.1. THAI+ configuration and dimensions of the system

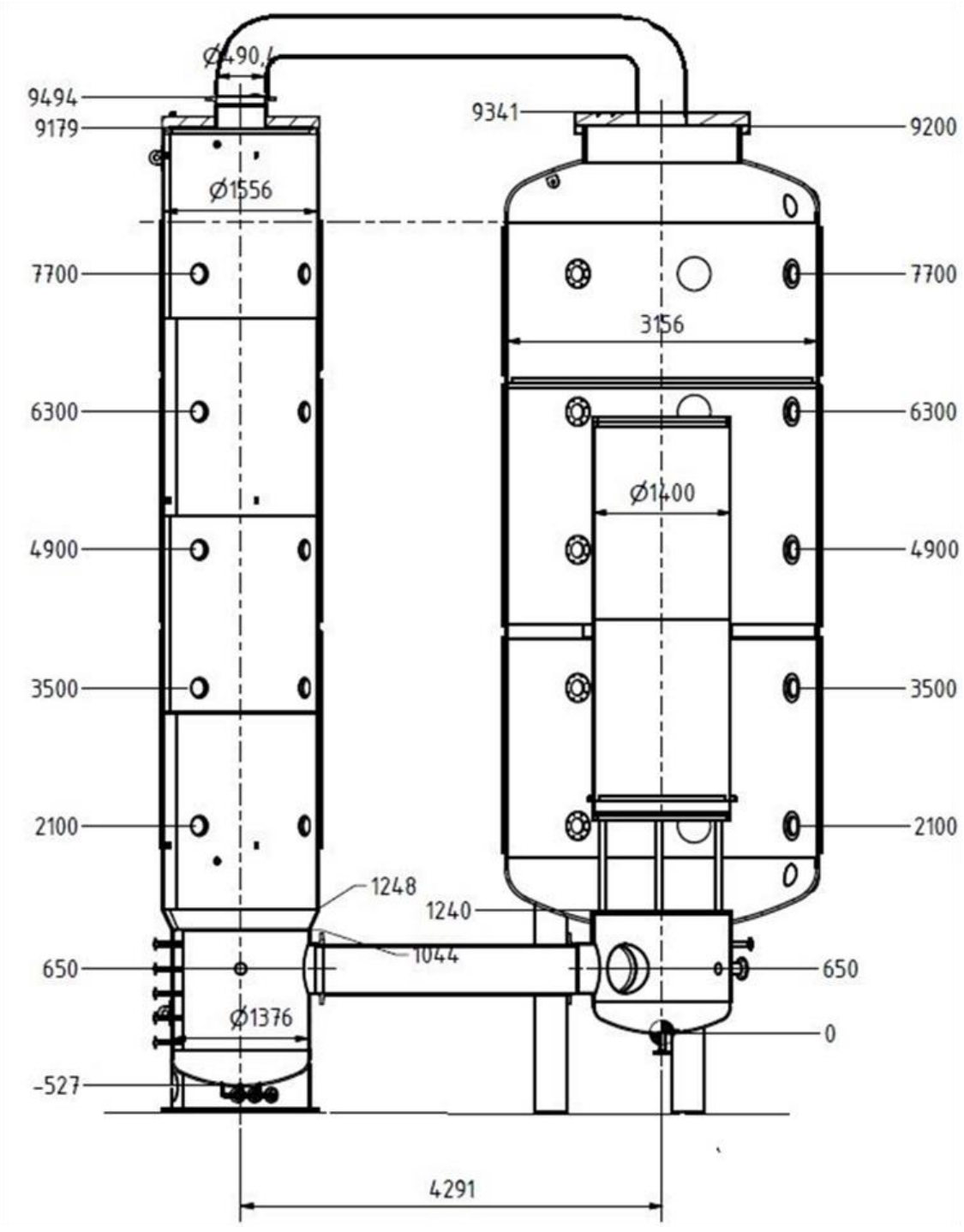

Source: Becker Technologies, 2020.

Figure 3.2. Arrangement of the two-vessel facility within the THAI building

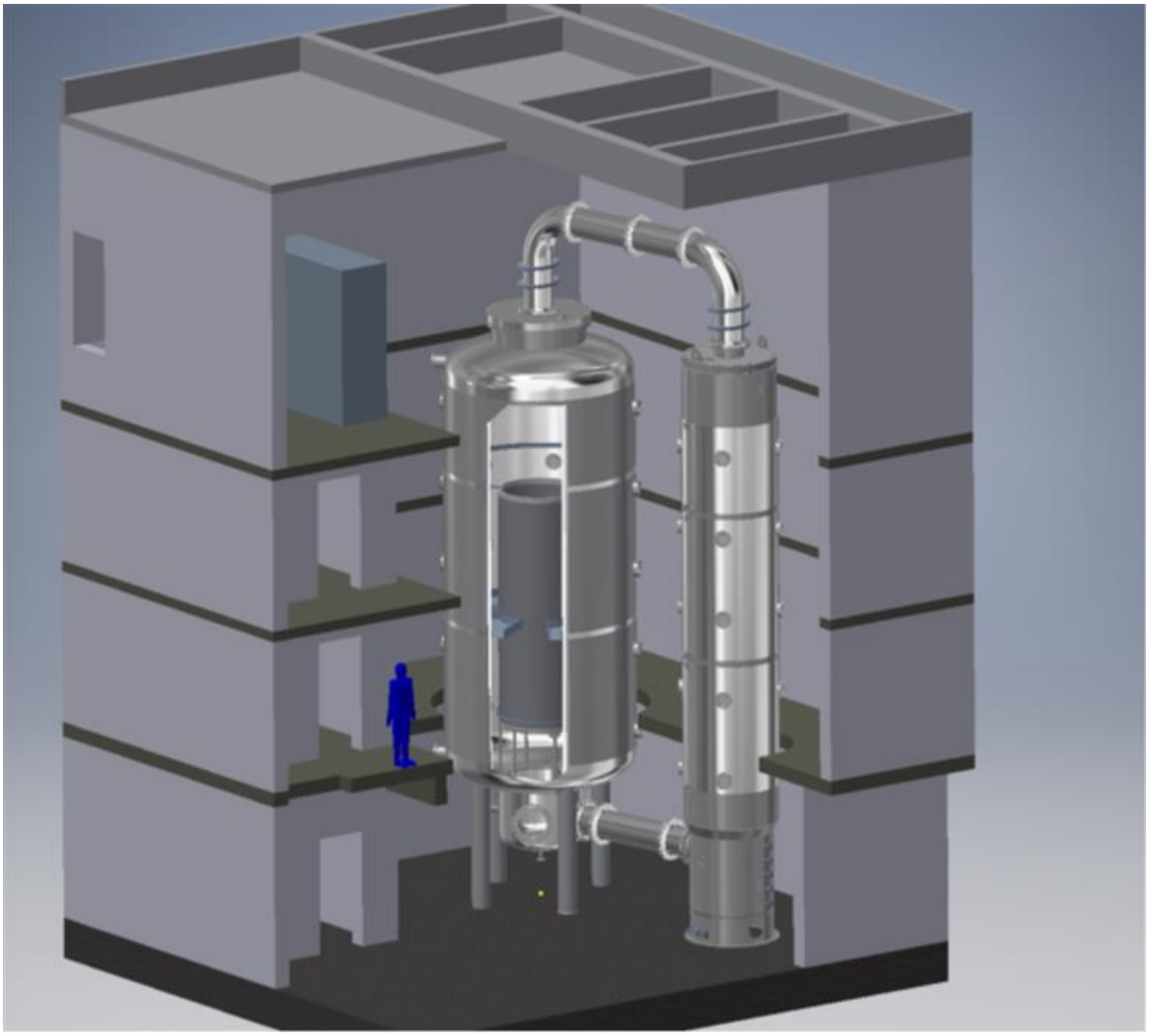

Source: Becker Technologies, 2020.

Figure 3.3. HD-40 to HD-45 test configuration: Position of igniters, supply systems, DN150 connection pipe and 3-bladed fan

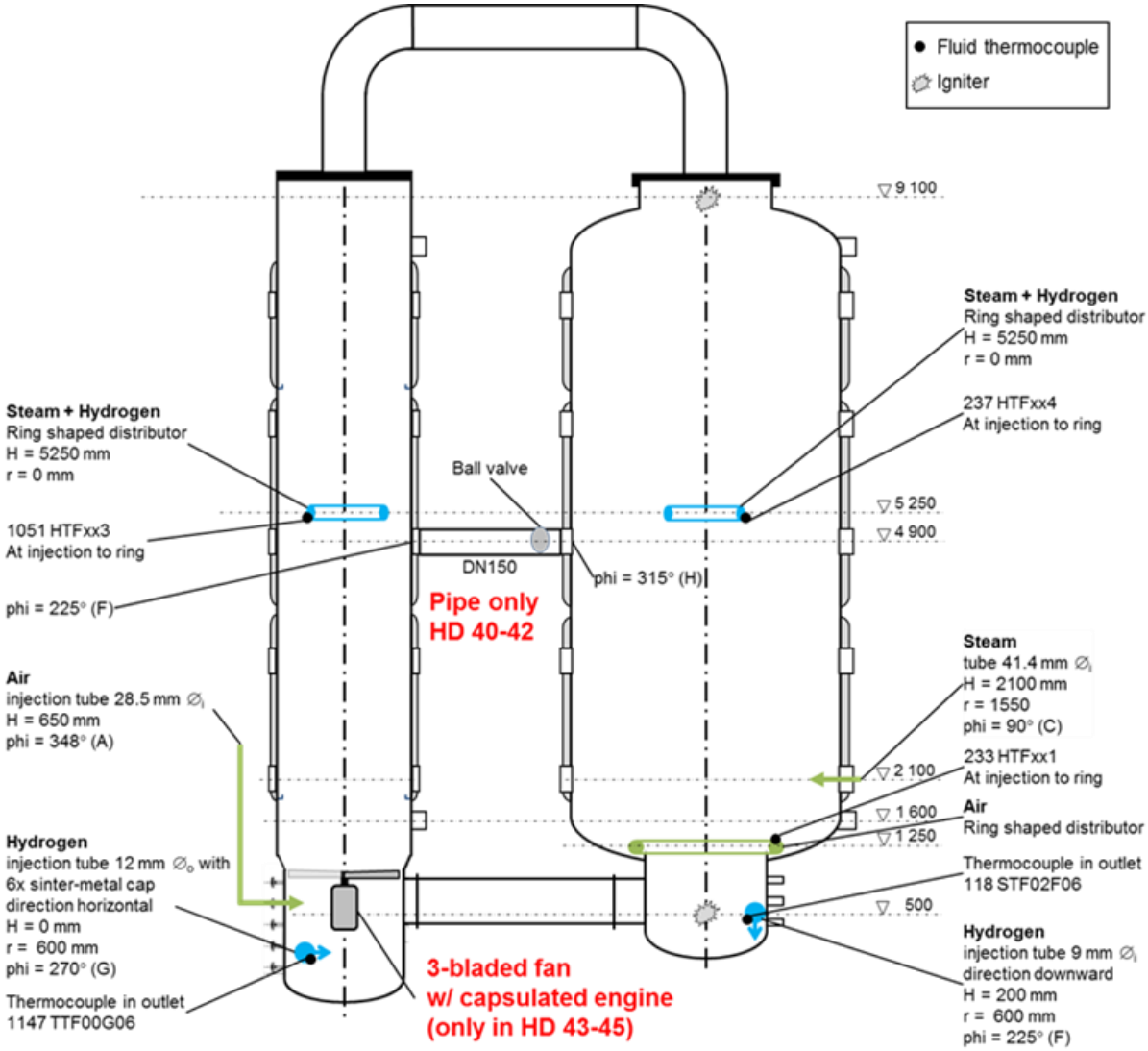

Source: Becker Technologies, 2020.

Figure 3.4. HD-43, HD-22 and HD-36: Pressure transient

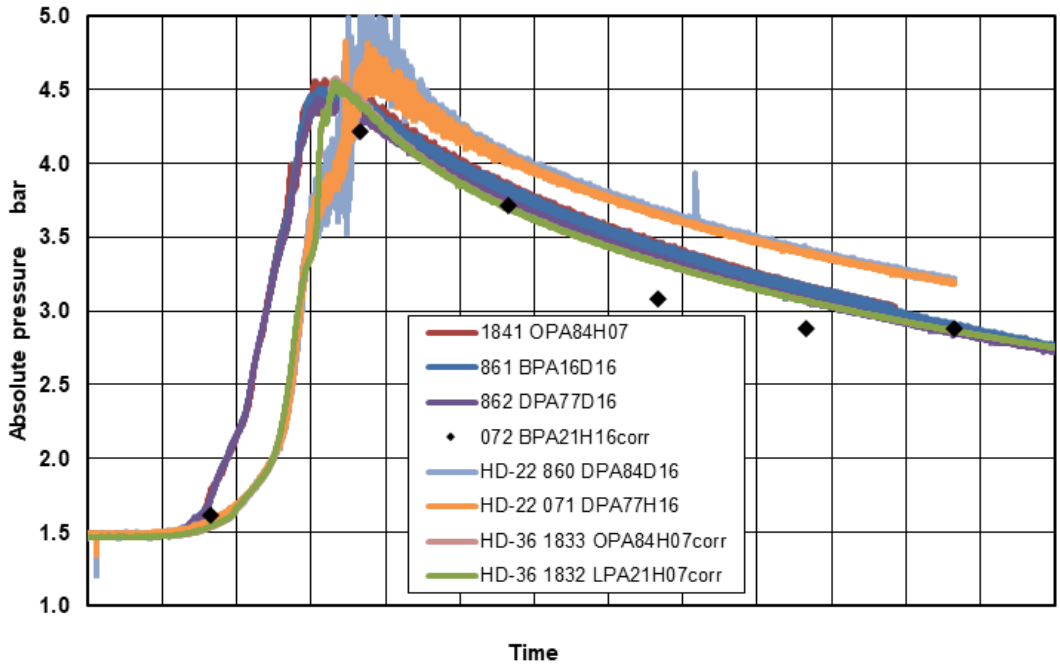

Source: Becker Technologies, 2020.

Figure 3.5. HD-43 to HD-45, HD-36, HD-22: Flame front propagation

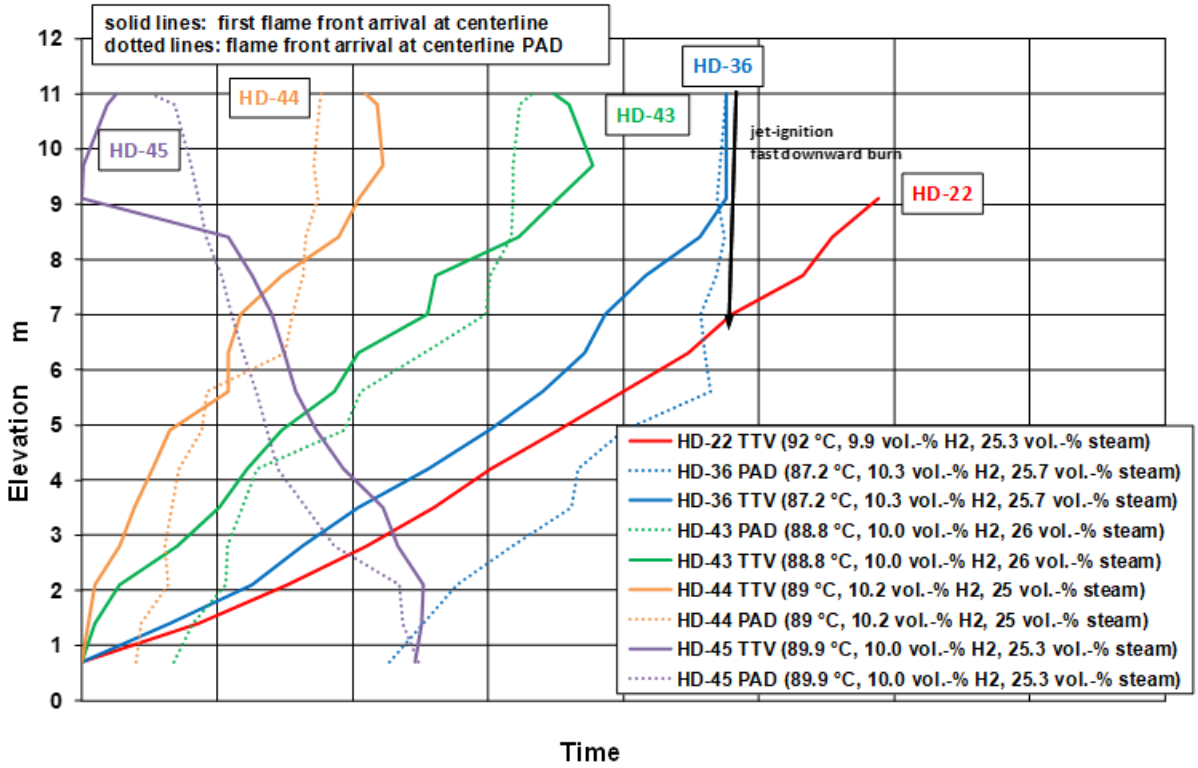

Source: Becker Technologies, 2020.

Figure 3.6. HD-36, HD-43 to HD-45: Peak pressures for different initial flows as function of volumetric flow. (peak pressures extrapolated to HD-44 with H2 concentration of 10.2 vol.-% using the slope of the AICC)**

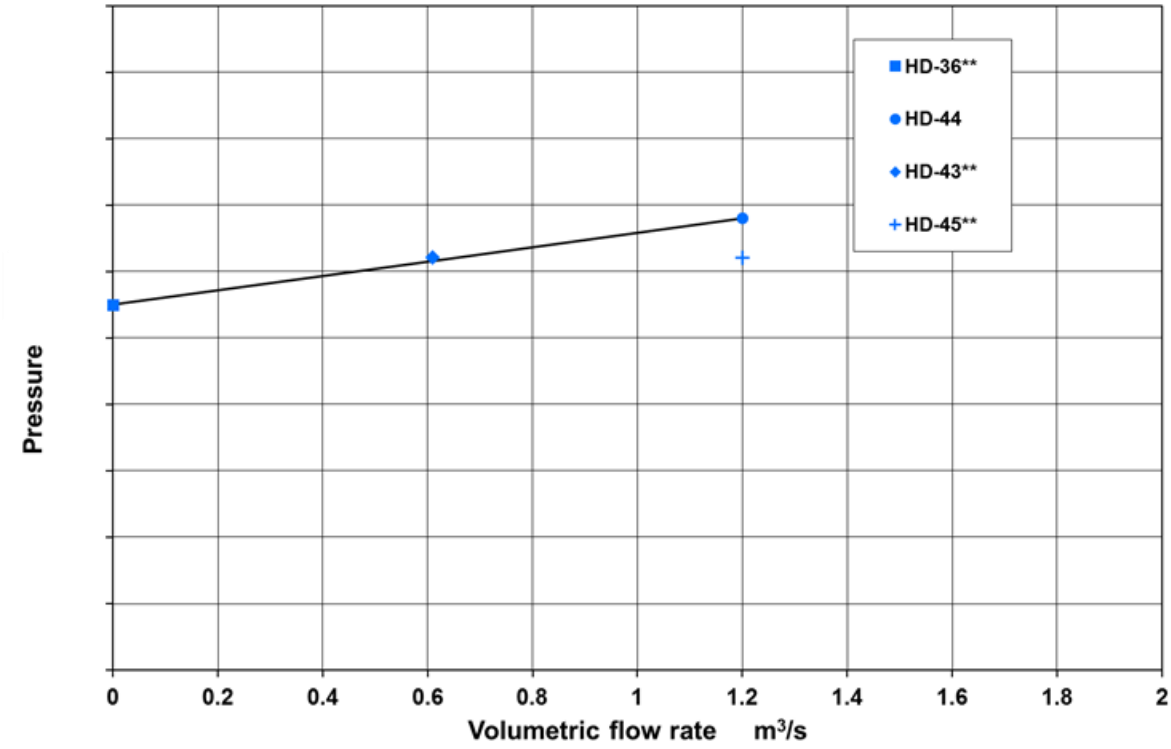

Source: Becker Technologies, 2020.

Figure 3.7. PAR unit (example NIS) and blower position. No blower was installed in HR-50.

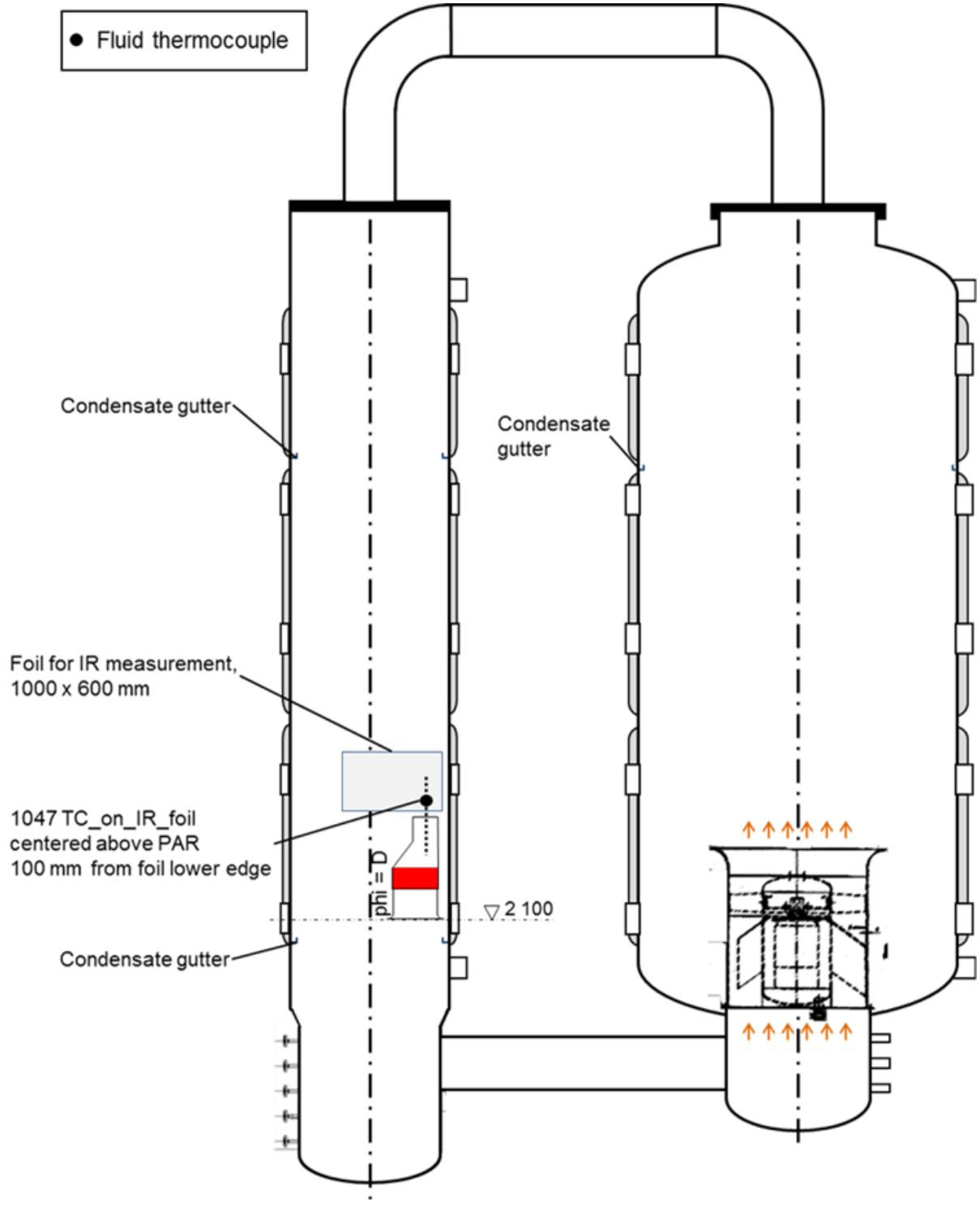

Source: Becker Technologies, 2020.

Figure 3.8. NIS PAR 1/8 module used in test HR-46 with 1 m chimney (left) and in test HR-47 with 0.25 m chimney (right)

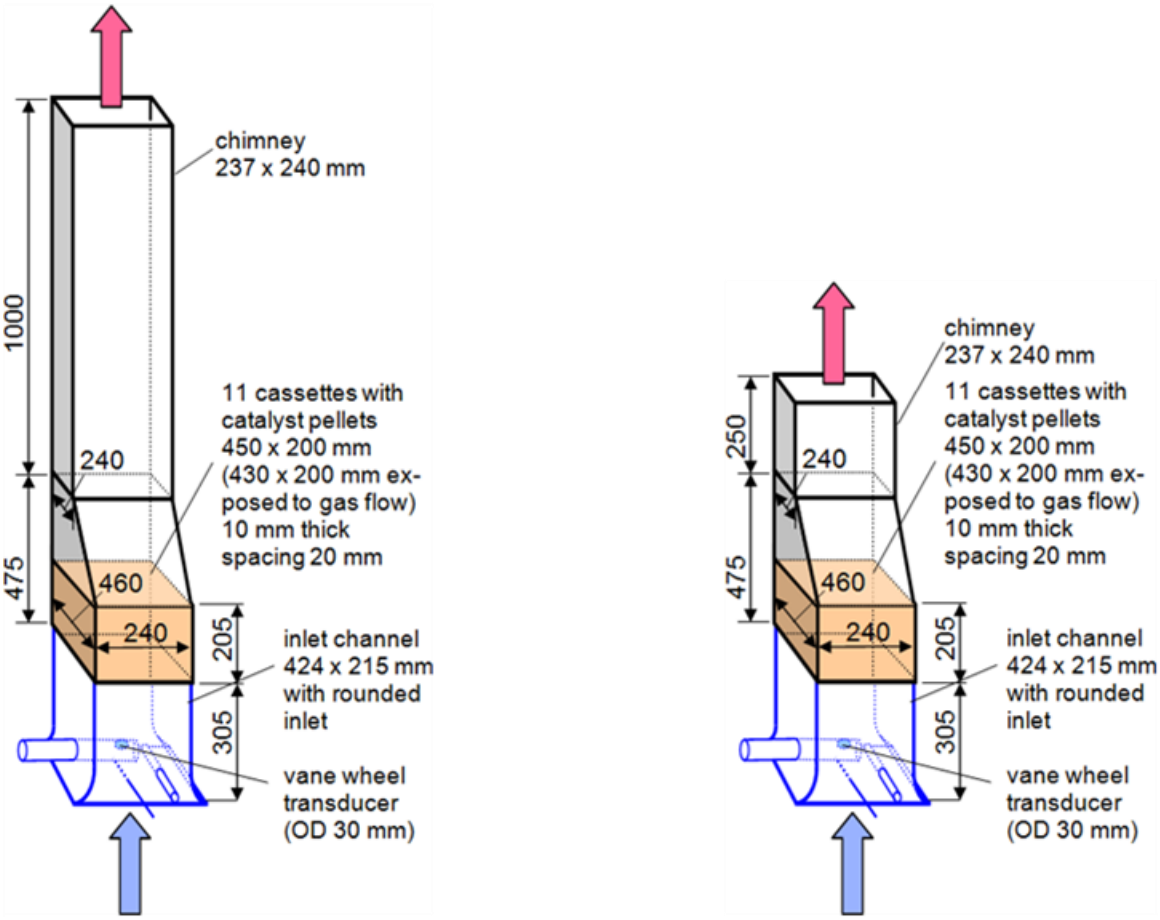

Source: Becker Technologies, 2020.

Figure 3.9. ½ FR-380 size AREVA PAR unit used in HR tests HR-48 to HR-50

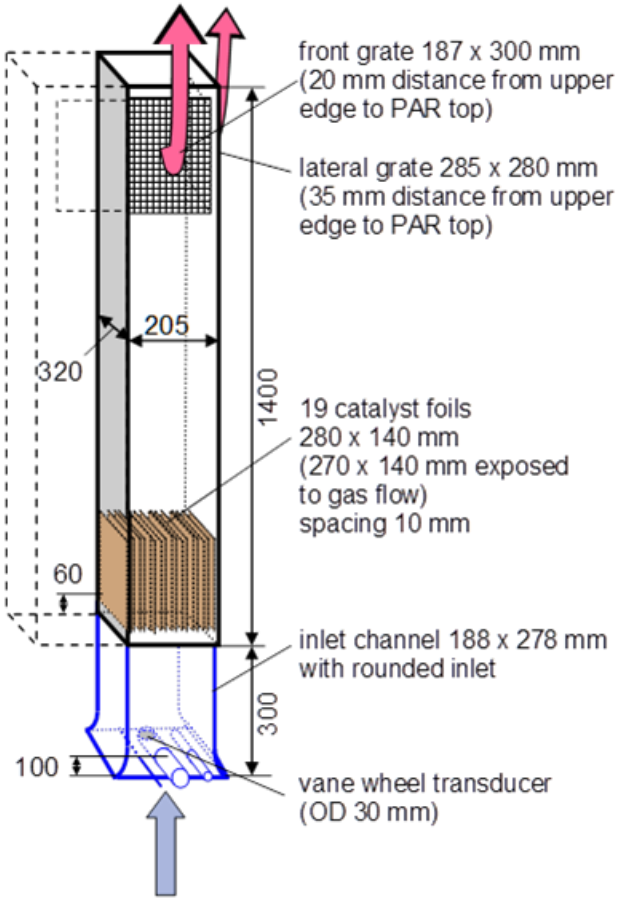

Source: Becker Technologies, 2020.

Figure 3.10. H2 depletion efficiency of NIS PAR tests HR-14, HR-15, HR-46, and HR-47

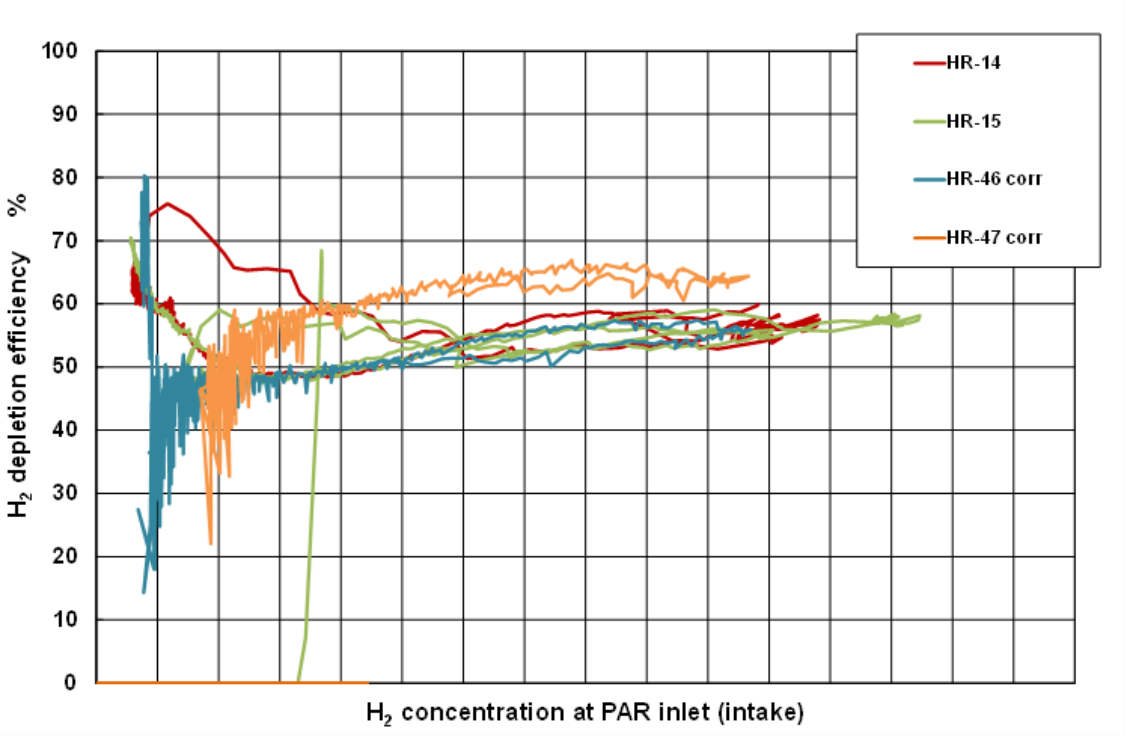

Source: Becker Technologies, 2020.

Figure 3.11. Recombination rate at the start-up of AREVA PAR tests HR-7, HR-8, HR-43 and HR-48

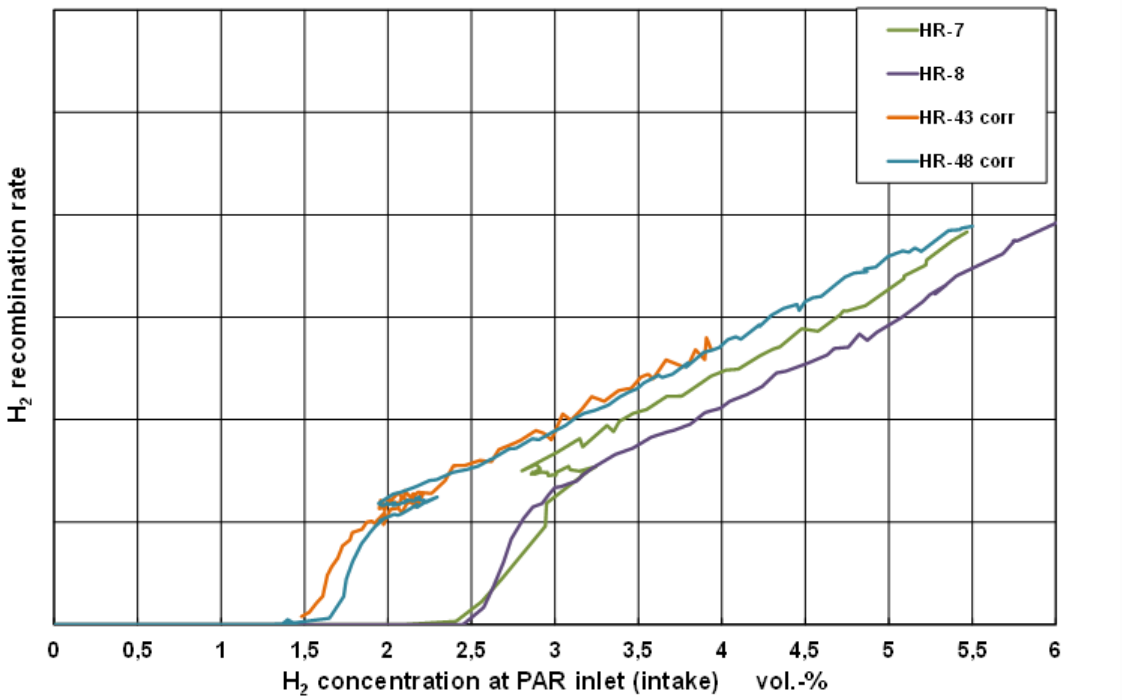

Source: Becker Technologies, 2020.

Figure 3.12. Depletion efficiency of AREVA PAR tests HR-7, HR-8, HR-43 and HR-48

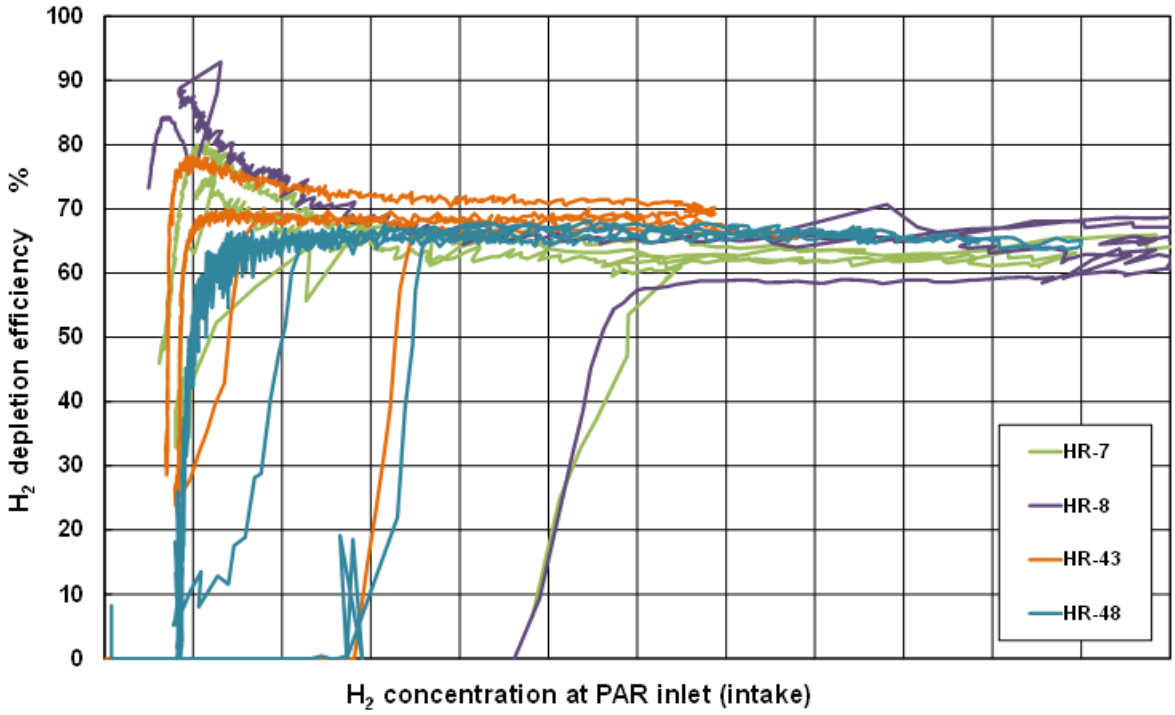

Source: Becker Technologies, 2020.

Figure 3.13. WH-24, WH-28: Gas injections and gas releases

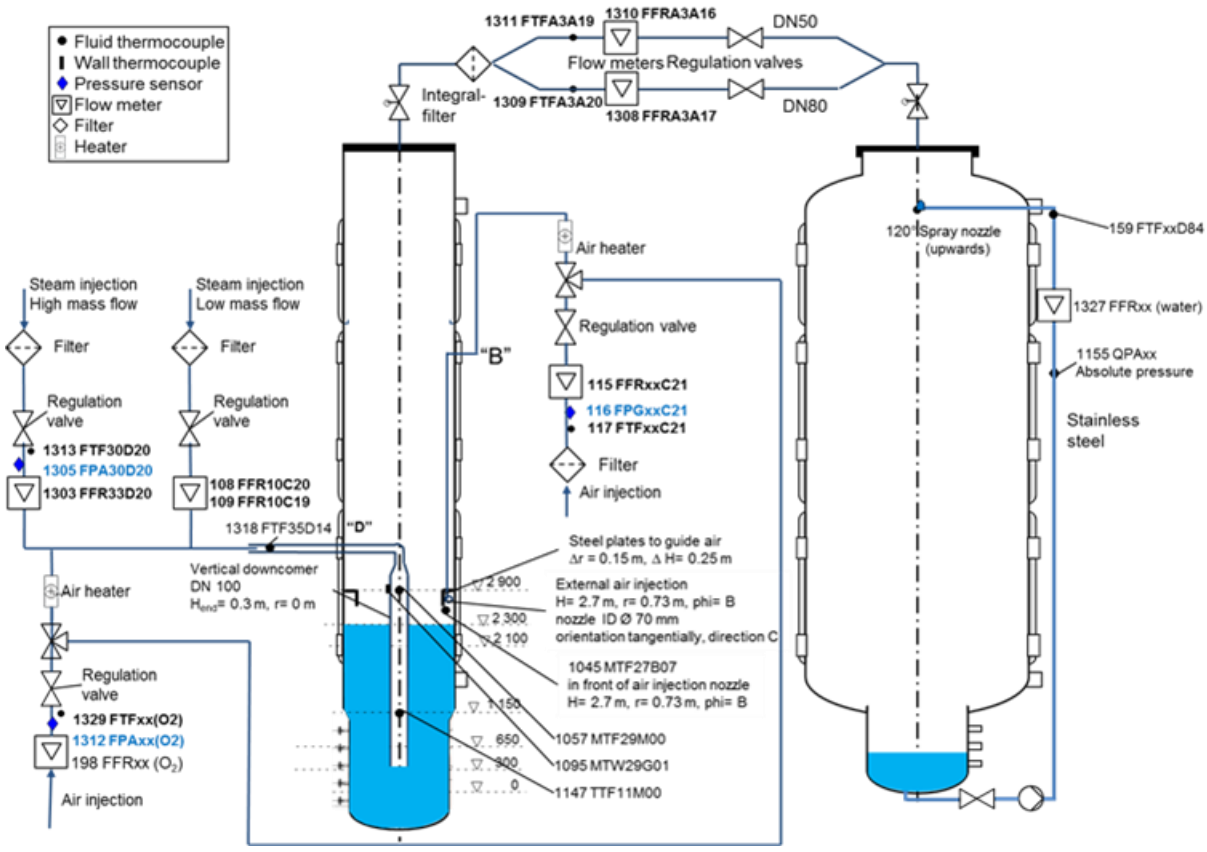

Source: Becker Technologies, 2020.

Figure 3.14. Primary bubbles leaving the downcomer during phases of low non-condensed volumetric gas flow, a3), a4) and b1)

Phase a3) Phase a4) Phase b1)

Source: Becker Technologies, 2020.

Figure 3.15. Initial bubbles leaving the downcomer exit, phases a1), a2), a5), b2), b3), and b4.

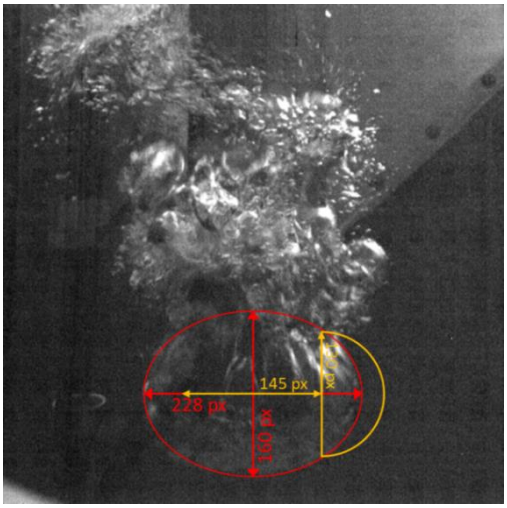

Ellipsoid a1): $r_1 = r_2 = 228$ px, $r_3 = 160$ px

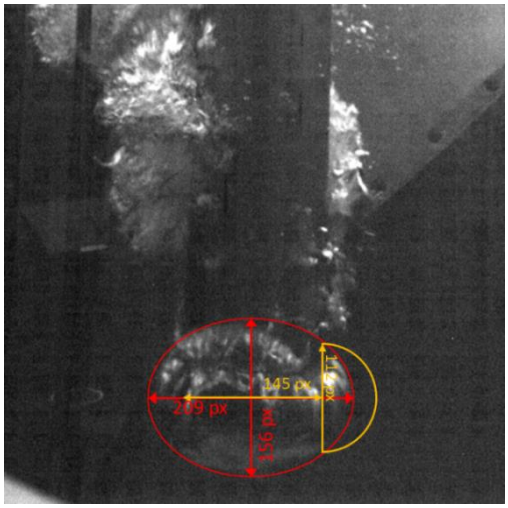

Ellipsoid a2): $r_1 = r_2 = 209$ px, $r_3 = 156$ px

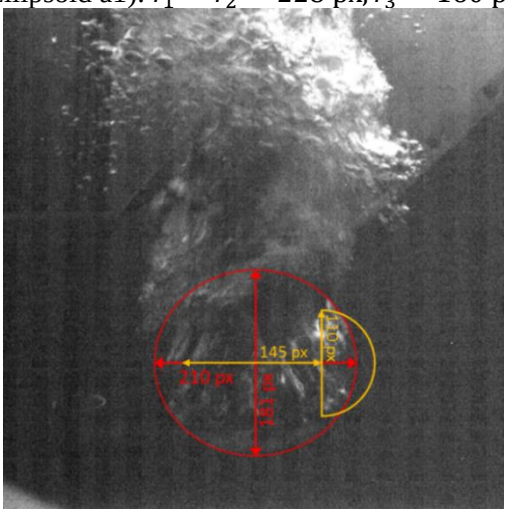

Ellipsoid a5): $r_1 = r_2 = 210$ px, $r_3 = 181$ px

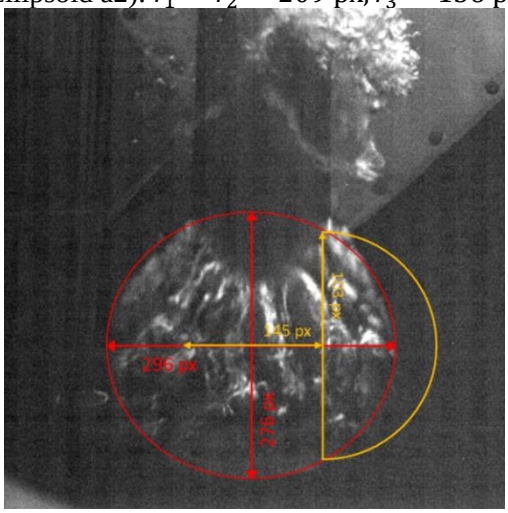

Ellipsoid b2): $r_1 = r_2 = 297$ px, $r_3 = 276$ px

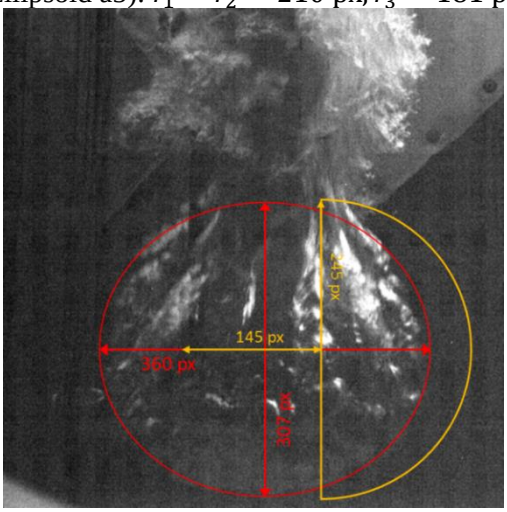

Ellipsoid b3): $r_1 = r_2 = 360$ px, $r_3 = 307$ px

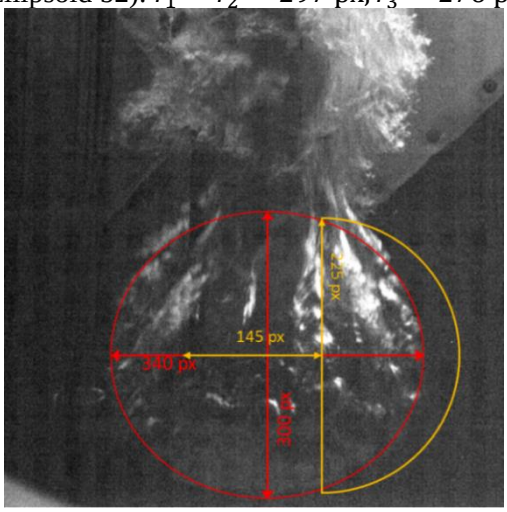

Ellipsoid b4): $r_1 = r_2 = 340$ px, $r_3 = 300$ px

Source: Becker Technologies, 2020.

Figure 3.16. Mass median diameter of particles as function of the superficial velocity, for boiling and subcooled pool conditions

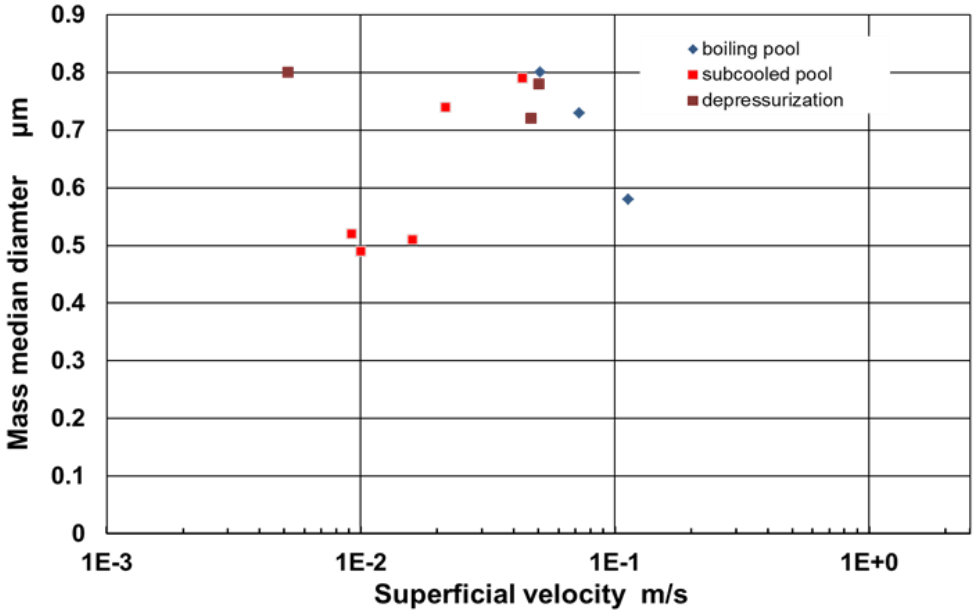

Source: Becker Technologies, 2020.

Figure 3.17. Average bubble diameters at ImgLow (H = 0.675 m) and ImgUpp (H = 2.125 m) in comparison to THAI tests WH7-WH15 measured 100 mm below the water surface

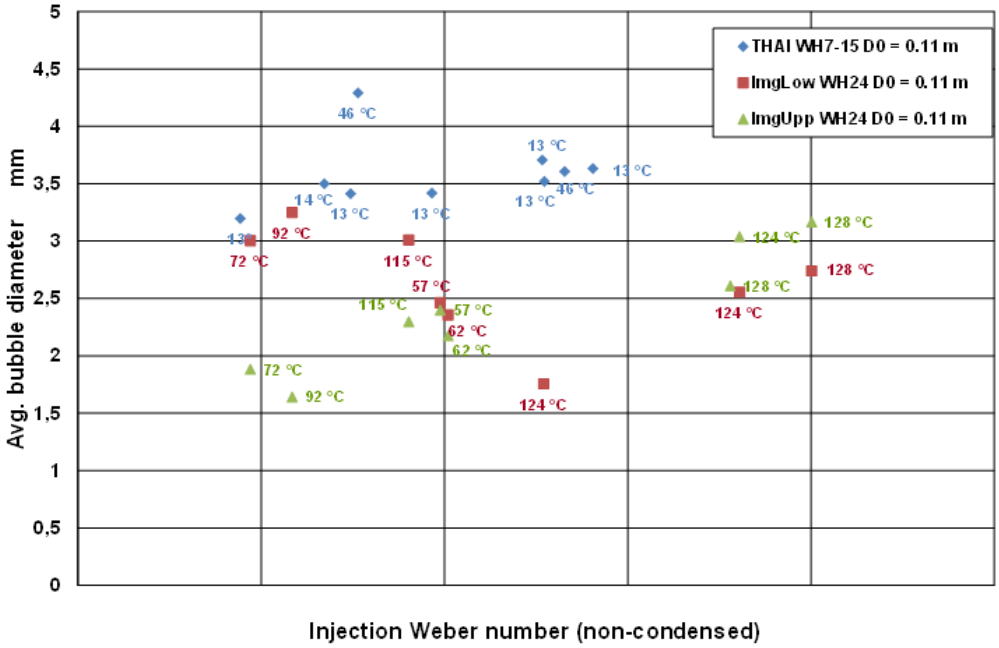

Source: Becker Technologies, 2020.

Figure 3.18. Iod-32: Gas injections and gas releases

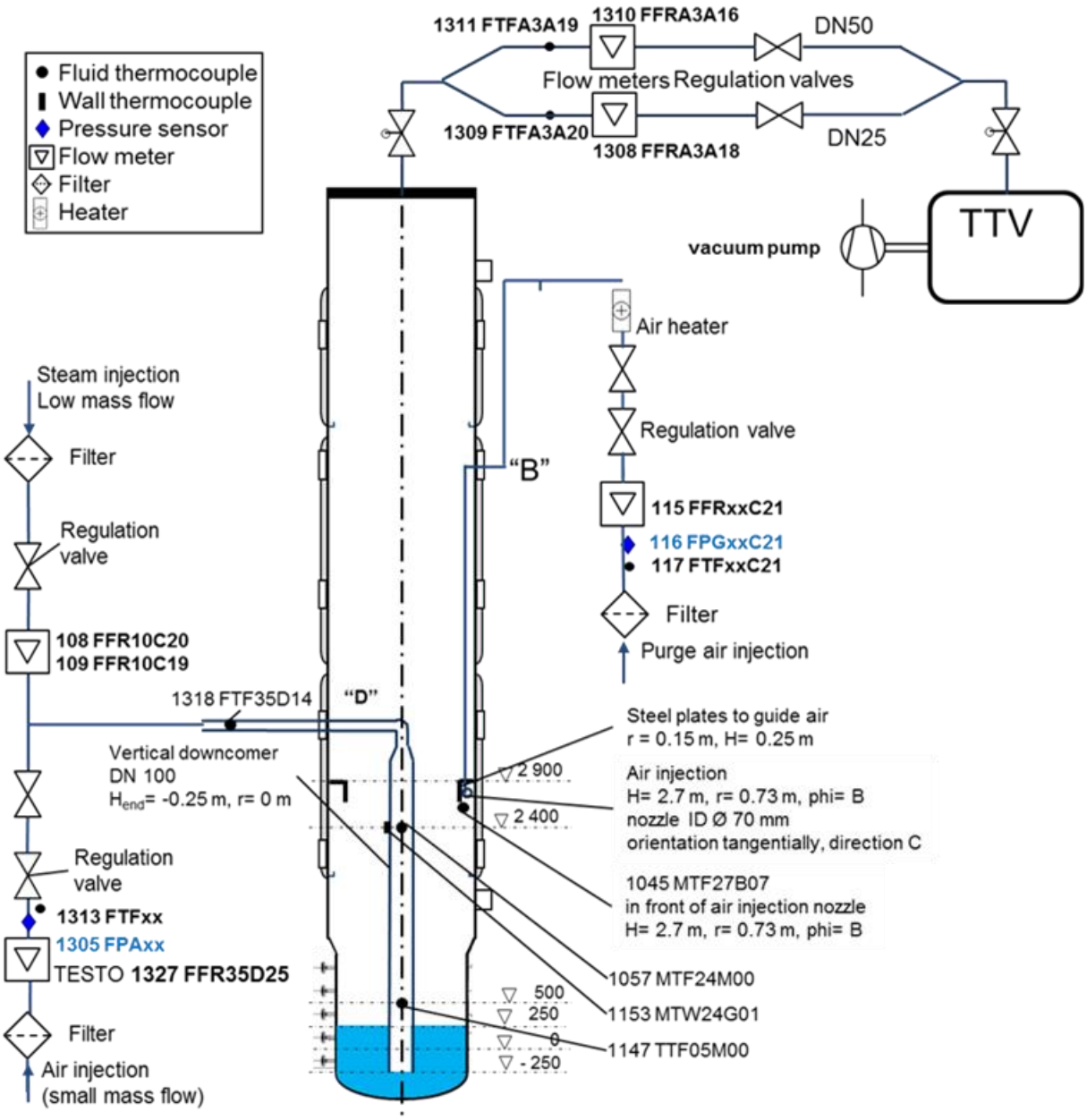

Source: Becker Technologies, 2020.

Figure 3.19. Iodine concentrations in PAD atmosphere

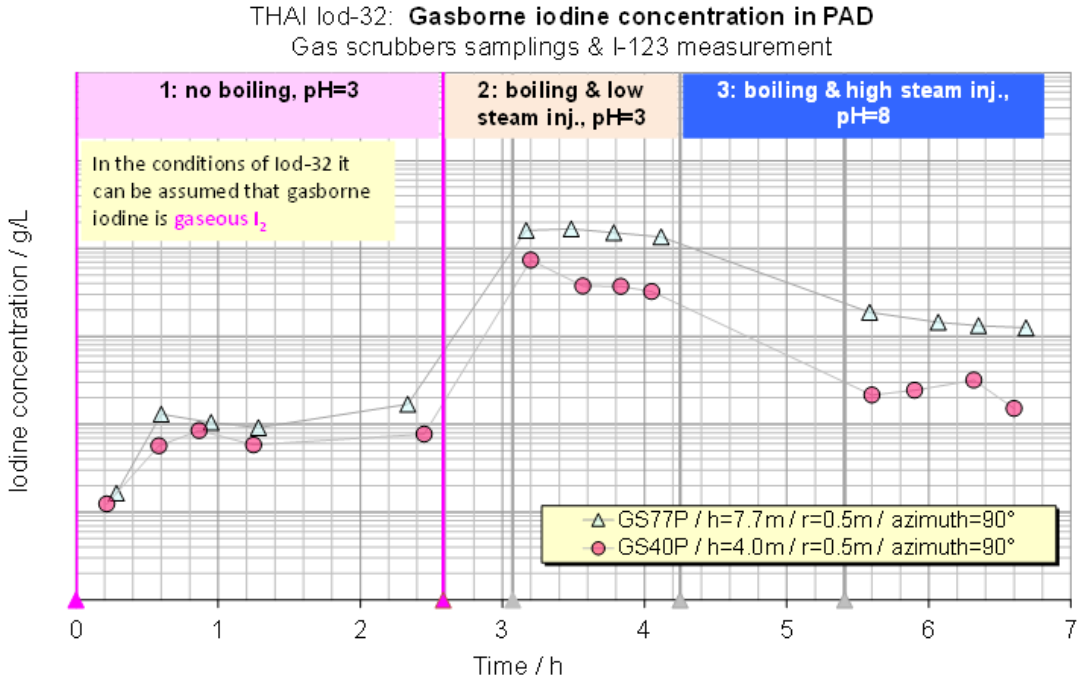

Source: Becker Technologies, 2020.

Figure 3.20. I_2 masses in PAD sump, measured data, down-scaled COCOSYS pre-test design calculation by GRS, and exponential fit to measured data

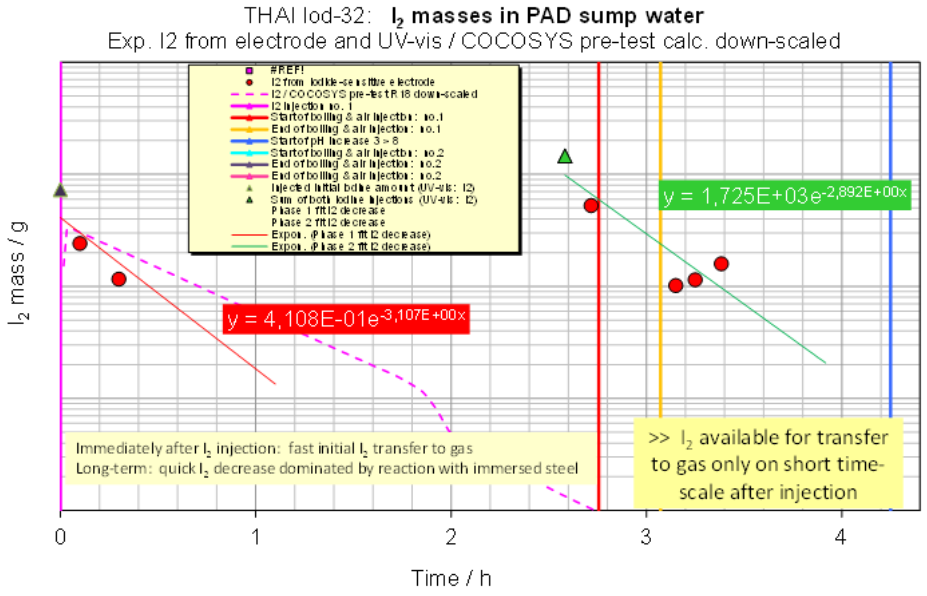

Source: Becker Technologies, 2020.

Figure 3.21. Iod-34: Test configuration: Iodine injection, sump recirculation, online radiation detectors, large painted surfaces and sampling stations

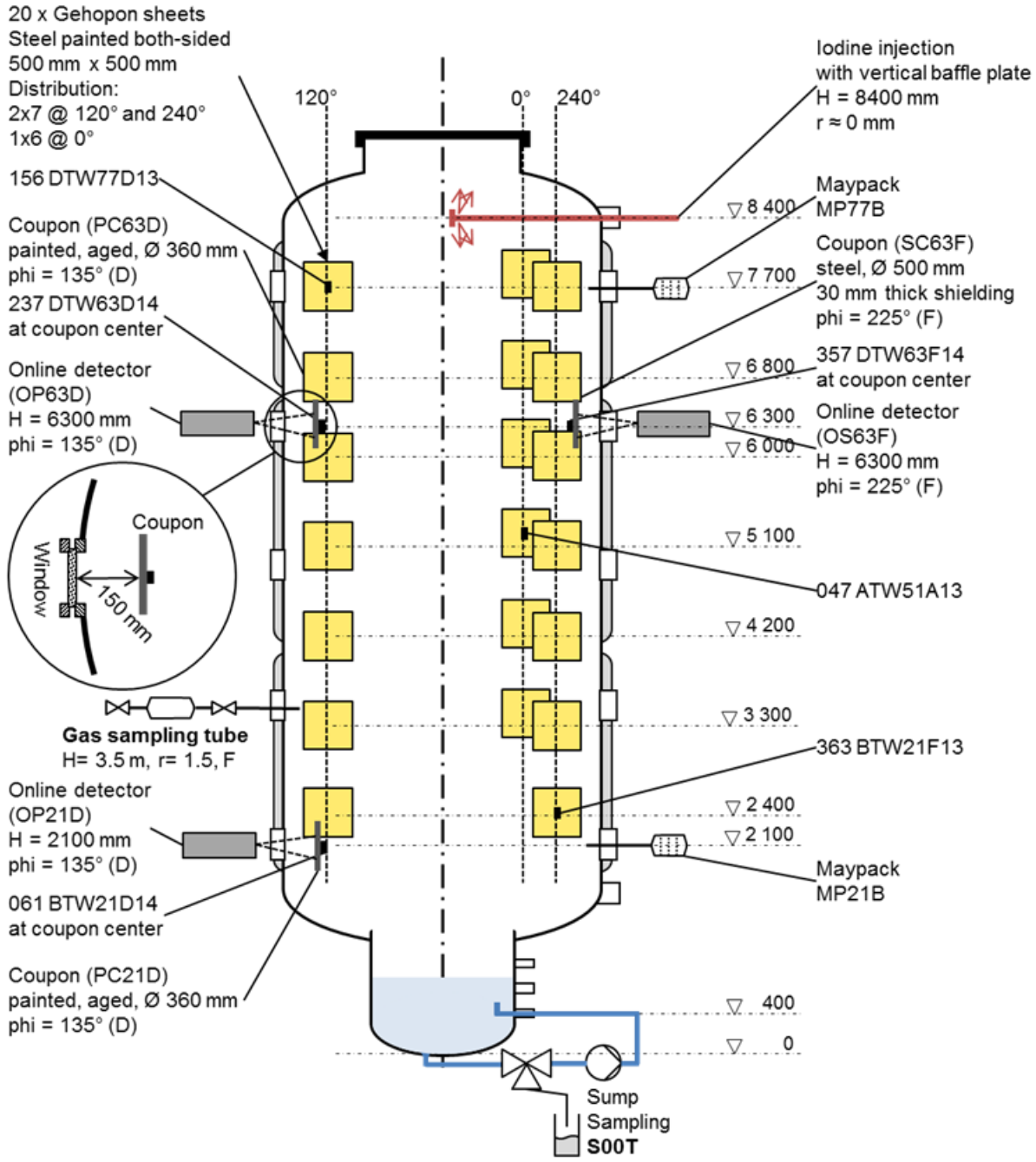

Source: Becker Technologies, 2020.

Figure 3.22. Iod-34: Photographs of painted coupons, comparison of surface degradation, before deflagration (left), after deflagration (right)

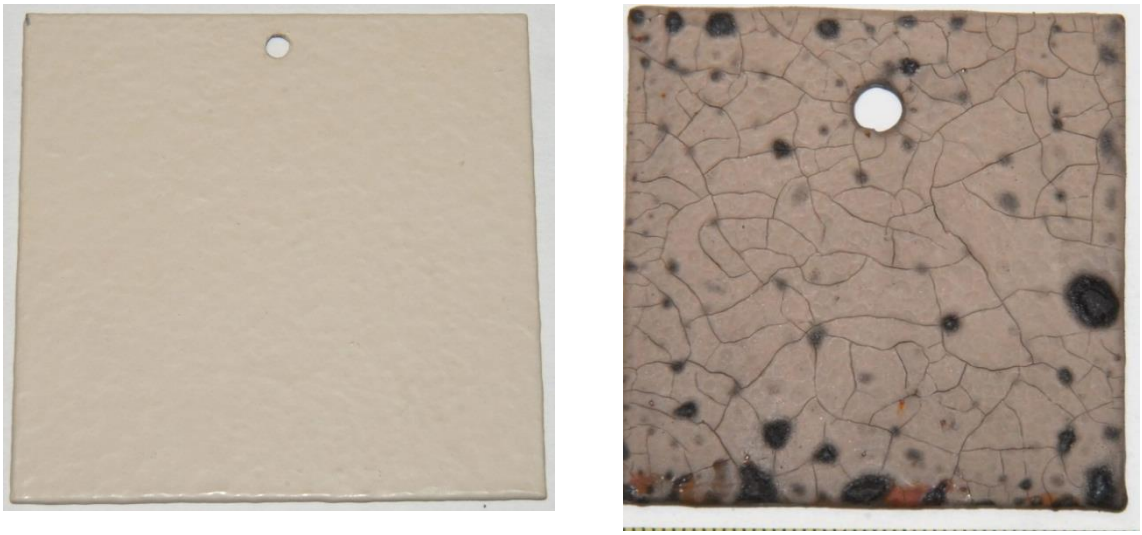

Source: Becker Technologies, 2020.

Figure 3.23. HD-46 test configuration: CsI injection, horizontal gratings, laser extinction measurement, aerosol sampling filter and impactor station

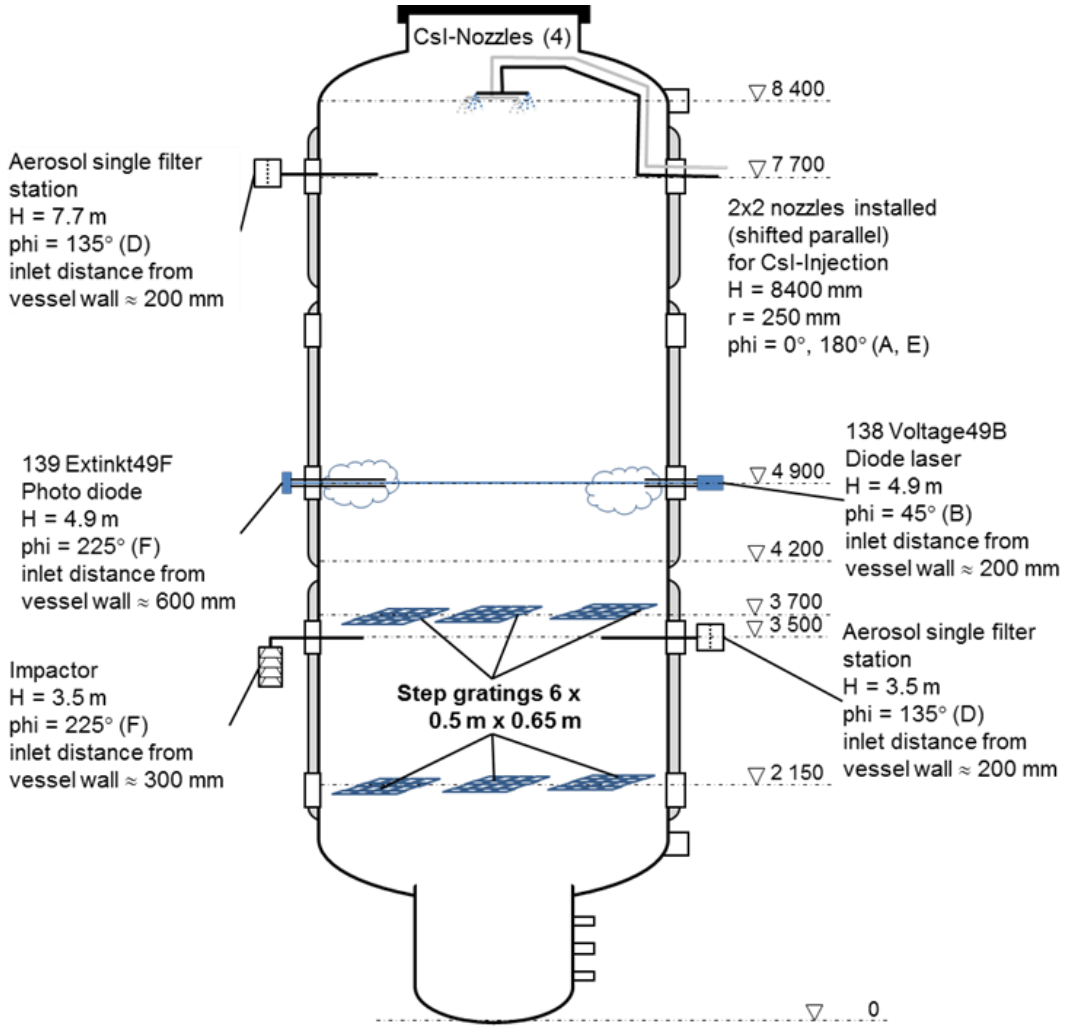

Source: Becker Technologies, 2020.

4. Conclusions

Conclusions were drawn from the results of the experiments conducted in the THAI/THAI$^+$ test facility regarding the following topics:

- Hydrogen deflagration (HD) tests in two-vessel geometry (HD 40-45);
- Hydrogen PAR tests (HR 46-50);
- Soluble and gaseous fission product (CsI, iodine) release from a boiling pool (WH-24, WH-28, Iod-32);
- Resuspension of iodine from paint by hydrogen deflagration (Iod-34);
- Resuspension of aerosol deposits from surfaces by hydrogen deflagration (HD-46).

4.1. HD experiments

The hydrogen deflagration test series consisted of six tests (HD40-45) performed in the two-vessel configuration (THAI$^+$) under uniformly mixed and stratified gas atmosphere conditions. The conclusions drawn from the results of the experiments HD-40 to HD-45 are listed below, and include the conclusions from the results of experiments performed previously in THAI/THAI$^+$ tests.

- During combustion, no pressure difference between the two vessels was observed, i.e. the two-vessel geometry behaved in this respect like a single vessel.
- Compared to the tests in the two-vessel facility, preceding tests performed in the single THAI vessel with the same initial conditions showed generally slightly higher peak pressures. This applies for both the well-mixed and stratified tests and even for tests with jet ignition-like combustion and has been attributed to an increased heat transfer due to the different surface/volume ratio (higher for the two-vessel facility). HD-42 is exceptional in this context due to noticeable pressure oscillation occurring inside the PAD, which leads to peak pressures being larger in the THAI+ configuration compared to the single THAI vessel.
- For the tests with a stratified atmosphere and upward burn direction, the comparison of single (THAI) and two-vessel tests (THAI$^+$) showed no unambiguous trend with respect to peak pressures. With respect to H_2 stratification, peak pressures were highest for the tests with homogeneous H_2 distribution (steam concentration and temperature still stratified). The reason is the higher mean H_2 concentration and the complete combustion in these tests. Any enhancing effect with respect to peak pressure, e.g. due to larger scale or interacting flame fronts in the two-vessel facility, was not determined.
- Combustion modes similar to jet ignition could be observed only in the two-vessel facility. In the tests HD-40, HD-41 and HD-36, it occurred always as a downward, fast combustion in the upper half of the PAD and was most pronounced for test HD-36, with average H_2 concentrations higher than for tests HD-40 and HD-41. In addition, test HD-36 exhibited the highest mean H_2 concentration (10.3 vol.-%) and the steam was superheated. It should be emphasised that to achieve a real jet ignition with a pressure increase higher in the downstream compartment than in the

ignition compartment, higher H_2 concentrations than those used in the present test series are required, as has been found by many other experiments conducted elsewhere.

- Flame acceleration was observed in the test series, particularly inside the lower and upper connection tube, caused by diameter change ahead of the expanding flame and increased turbulence in the connecting pipes. The most pronounced flame acceleration occurred in the lower connecting pipe in test HD-41 (H_2 concentration 12 vol.-% in the pipe, quasi no steam, relatively low temperature), with a flame speed of approximately 50 m/s.
- For some of the tests, a flow velocity of up to 7.5 m/s in the interconnecting pipes and up to 0.3 m/s in the PAD was established prior to ignition. This flow produced significant initial turbulence in the interconnecting pipes, with an associated high flame speed in the pipes even opposite to the initial flow direction. Peak pressures increased slightly with flow velocity. The comparison to a test with the same initial conditions, but without initial flow, revealed a higher flame speed in the upper interconnecting pipe with downward-directed jet ignition into the upper half of the PAD, i.e. the influence of an initial flow on combustion behaviour is noticeable.

4.2. HR experiments

Five tests (HR-46 – HR-50) were conducted to investigate the effect of counter-current flow conditions on PAR performance behaviour. The flow loop with a magnitude of 0.5 m/s to 1 m/s in the vicinity of the PAR was established with a blower. For tests HR-46 and HR-47, an NIS $1/8^{th}$ module PAR was installed inside the PAD vessel and for tests HR-48 to HR-50 an AREVA FR-380 PAR was installed, which was reduced to half of the number of catalytic foils of the actual PAR. The main results are summarised below:

- Generally, the test results indicate that the AREVA PAR with top cover on the chimney (lateral outlets) provided effective means to protect the PAR from intrusion of counter-current flow within the range of investigated conditions whereas the NIS PAR with an open-ended outlet without top cover was prone to intrusions of counter-current flow in case of low H_2 concentrations.
- In case of AREVA PAR, counter-current flow had no measurable impact on the performance behaviour under the investigated conditions.
- Large convection loops inside the $THAI^+$ facility were effective measures to transport the hydrogen from its release location towards the recombiners.
- Comparing the test results of HR-46 and HR-47 with initially counter-current flow conditions and of the previous HR tests (initially quiescent) using the NIS PAR under similar thermodynamic boundary conditions revealed that the first onset of hydrogen recombination was much faster under conditions of counter-current flow. However, the recombination rate was significantly reduced as long as the hydrogen concentration remained below about 2-3 vol.-%, due to an initially stable downward flow and later oscillations of the flow direction inside the PAR. For higher hydrogen concentrations, the recombination rate and hydrogen depletion efficiency of the NIS PAR are in agreement with those determined earlier in initially quiescent THAI HR-experiments. The shortening of chimney height resulted in a reduced PAR internal flow, which could be explained by the reduced buoyancy induced chimney flow. For test HR-47 (NIS PAR), with reduced chimney height, the efficiency increased by about 10% due to a reduced internal

gas velocity, which in turn increased the residence time of the hydrogen at the catalytic cartridges.

4.3. Soluble and gaseous fission product (CsI, iodine) release from a boiling pool

Three tests were conducted to investigate wet resuspension or re-entrainment of aerosols (WH-24 and WH-28) and the release of volatile gaseous iodine (Iod-32) from a water pool under boiling conditions. The gas superficial velocity was in the range of 0.01 to 0.12 m/s.

In the WH-24 test, aerosol re-entrainment was quantified based on the concentrations of CsI particles released from the sump within a total of 12 test phases using injection of air, steam and a mixture of steam and air injection through a scaled down DN 100 downcomer pipe into the vessel sump. The investigated test conditions included aerosol release from a pool under subcooled conditions at a broad range of pool temperatures and during flashing due to depressurisation. The sump of the vessel was filled with about 4.6 m^3 of water in which 10 g/L caesium iodide was dissolved as a representative fission product. The vessel walls were heated to 138°C to provide a superheated atmosphere, which was necessary to dry the aerosol particles released from the sump by entrained water droplets. The aerosol released from the sump into the gas space has was measured independently by using two sampling filters, a large integral filter and two gas scrubbers. The size distribution of the aerosol particles was determined using a low-pressure cascade impactor, resulting in small particles. These particles remain airborne in the long term and will be of relevance for the prediction of a potential radiological source term.

The gas release and the behaviour of the bubble column were measured by high-speed digital imaging. Digital data processing was applied to evaluate the bubble formation frequency, the bubble break-up and the terminal velocity of the gas bubbles below the water's surface. The bubble diameter below the pool surface was found to increase with the injection Weber number from about 1.5 mm for low injection gas flows up to 3 mm for high steam injection mass flows. The image processing of the bubble column width was used to approximate the superficial velocity based on the area through which the gas bubble break-through will occur at the pool surface.

The entrainment calculated from the aerosol measurements was in accordance with previous experimental findings obtained in the THAI facility and other test facilities. Entrainment values were between $E = 5 \cdot 10^{-6}$ and $E = 7 \cdot 10^{-5}$ in test WH-24. The entrainment in WH-24 initially increased with superficial gas velocities but decreased for even larger superficial velocities belonging to the transition and churn turbulent flow regime.

Deviating from test WH-24, for test WH-28 the surface tension of the water was reduced by adding surfactant and antifoaming emulsion to suppress the foaming tendency of the liquid. The reduction of the surface tension in WH-28 favoured the release of larger particles compared to WH-24, but on the other hand a high number of tiny particles were also released, generating bimodal distributions.

The entrainment calculated from the aerosol measurements in tests with surfactant was about one order of magnitude larger compared to the de-mineralised water of test WH-24. In test WH-28, entrainment values during different test phases varied between $E = 3 \cdot 10^{-6}$ and $E = 3 \cdot 10^{-3}$. The overall highest entrainment rates were obtained in the bubbly flow regime whereas the entrainment decreases for large superficial velocities corresponding to the transition and churn turbulent regime.

Results from different particle measurement techniques that were used to evaluate the entrainment in tests WH-24 and WH-28 indicate that the absolute entrainment is subject to uncertainty by a factor of 2 – 5.

Test Iod-32 was performed to study the release of volatile iodine from a boiling sump. The test was run in the PAD vessel, using the THAI vessel as a pressure relief tank.

At the start of a reference phase in non-boiling conditions, 0.73 g of molecular iodine (I_2) radio-labelled with I-123 was injected into the sump water (V = 1.09 m³) of the PAD, and a small amount of I_2 was released to the PAD atmosphere within 2.5 hours. The great majority of the aqueous I_2 was converted into non-volatile iodine by reaction with the steel wall of the sump. This I_2 depletion was limiting the I_2 releases from the sump.

Before starting the second test phase, another 0.73 g I_2 was injected into the PAD sump (V = 1.09 m^3). Boiling was induced by a 5 min depressurisation and maintained by steam injection into the sump water. The gas atmosphere from the PAD was vented to the TTV during both the depressurisation and the steam injection phases. This led to a release of I_2 from the sump water: the I_2 release was ten times higher compared to the non-boiling conditions in the reference phase.

The I_2 concentration in the gas was higher by a factor of 100 after boiling, compared to the end of the reference phase. The online detectors indicated a stronger I_2 release upon depressurisation compared to the I_2 release induced by steam injection into the boiling sump water.

4.4. Resuspension of iodine from paint by hydrogen deflagration

Test Iod-34 studied the resuspension of iodine from surfaces coated with decontamination paint by a hydrogen deflagration, where the paint was pre-loaded with iodine in a representative manner. The reference test for hydrogen deflagration was the THAI test HD-22 conducted in the framework of the NEA THAI project.

In the first phase of the test, I_2 (1 g) was injected into the THAI vessel at a temperature of about 90 °C and a steam concentration about 25 vol.-%. Within 5 hours, the gaseous I_2 was decreased to a level of less than 1% due to deposition onto painted surfaces and steel walls.

In a second test phase, the unwanted but inevitable I_2 deposition on steel walls of the THAI vessel was washed off with three sprayings of fresh, decalcified water and the washed iodine was removed from the THAI into the PAD vessel.

Prior to the H_2 deflagration, the gas phase iodine concentration was practically free of iodine. The deflagration produced peak gas temperatures above 900 °C. The iodine release from paint into the vessel atmosphere was measured using gas scrubbers (total gas-borne iodine), Maypack filters (iodine in aerosol form, molecular iodine, organic iodide) and online monitoring of the iodine loadings on deposition coupons. SEM/EDX analyses and microscopy of used and unused paint coupons were performed to characterise the paint degradation due to H_2 deflagration.

The H_2 deflagration induced a significant iodine release from the surfaces to the gas phase. The iodine release fraction amounts to a range between 4 and 9% of iodine inventory pre-deposited before H_2 deflagration, considering experimental uncertainties of the initial iodine loadings on the painted and steel surfaces. Out of the resuspended amount, 50% of the iodine released by H_2 deflagration was in the form of gaseous organic iodide.

The H_2 deflagration strongly degraded the painted surfaces, which showed a flaky structure, including blistering, cracks and craters. Degradation was approximately similar over the

whole THAI vessel and increased at the edges of the painted coupons. Consistent with paint degradation, significant aerosol concentration in the gas atmosphere was observed visually.

4.5. Resuspension of aerosol deposits from surfaces by hydrogen deflagration

The objective of test HD-46 was to study the resuspension of aerosols that were deposited on vertical, horizontal and containment-typical step grating surfaces and the thermal decomposition of CsI particles by hydrogen deflagration.

In the first phase of the test, CsI particles (242 g) were injected into the THAI vessel and characterised by measuring the airborne particle concentration and their size distribution. Within 29 h after the aerosol release into the vessel, at least 99.5% of the injected CsI mass was deposited onto the walls. Thereafter, an ignitable gas mixture (1.47 bar, 89.7°C, 23.6 vol.-% steam, 10.1 vol.-% H_2) was established in the vessel.

The hydrogen deflagration, with peak pressure of almost five bar and peak gas temperatures above 900 °C, resuspended about 4% of the previously deposited CsI, which settled much more slowly.

In addition to particle resuspension, the release of gaseous iodine by thermal decomposition of CsI particles due to the high temperatures during hydrogen deflagration was measured by using GSs. Aerosol filters were installed upstream of the GS to discriminate iodine in gaseous form from iodine in aerosol form. The mass ratio of gaseous iodine relative to the particulate CsI was about 1% in the first gas scrubber measurement after the deflagration event. The I_2 concentration decayed rapidly due to the physisorption of gaseous I_2 on CsI particles or the steel walls of the vessel. The corresponding conversion factor that quantifies the thermal decomposition of CsI by relating the released molar concentration of gaseous iodine to the initial molar concentration of CsI is about 2%.

References

Brown, M.L., E.C. Beahm and W.E. Shockley (1990), *The Oxidation of Cesium Iodide in Stationary Premixed Hydrogen Flames*, Advanced containment experiments report ACE-TR-B6, ORNL/M-1080, Oak Ridge National Laboratory, Oak Ridge, TN, 1990.

Balewski, B., S. Gupta and K. Fischer (2011), "Water Flow with Bubble Columns - Boiling Water Reactor Experiments *WH-7 to WH-152*", Report 1501361–WH-7-15-FB/TR, Becker Technologies GmbH, Eschborn, Germany, October 2011.

Deschamps, F. and J.C. Sabroux (2003), "Particulate Iodide to Gaseous Iodine Conversion in a Passive Autocatalytic Recombiner", *J. Aeros. Sci.*, Vol. 34, pp 1087-1088, 2003.

Freitag, M., A. Kühnel and G. Langer (2016), "Erweiterung der THAI-Anlage durch einen zweiten Druckbehälter: THAI$^+$ - Extension of the THAI test facility by a second vessel: THAI$^+$", Technical Report 1501455-FB/TR-THAI$^+$, Becker Technologies GmbH, Eschborn, Germany, May 2016.

Freitag, M., E. Schmidt, M. Colombet, von Laufenberg, B., A. Kühnel and S. Gupta (2016), "Rekombinator in Gegenströmung", HR-43 to HR-45, Technical Report 1501455-TR-HR43-45, Becker Technologies GmbH, Eschborn, Germany, August 2016.

Freitag, M., B. von Laufenberg and E. Schmidt (2017a), "Hydrogen Deflagration Tests in a Two-Vessel Test Facility Test series HD-36 – HD-39", Technical Report 1501455 – TR – HD36-39, Becker Technologies GmbH, Eschborn, Germany, March 2017.

Freitag, M., B. von Laufenberg and E. Schmidt (2017b), "Re-Entrainment of Fission Products from Water Pools at Elevated Temperature – Test WH-24", Technical Report No. 1501516 – TR – WH-24, Becker Technologies GmbH, Eschborn, Germany, December 2017.

Freitag, M., B. von Laufenberg and E. Schmidt (2017c), "Hydrogen Deflagration Tests in a Two-Vessel Test Facility Test series HD-36 – HD-39", Technical Report 1501455 – TR – HD36-39, Becker Technologies GmbH, Eschborn, Germany, March 2017.

Freitag, M. and E. Schmidt (2017), "Passive Autocatalytic Recombiner Operation under Counter Current Flow Conditions - Test series HR-46- HR-50", Technical Report No. 1501516 – TR – HR-46 – HR-50, Becker Technologies GmbH, Eschborn Germany, June 2017.

Freitag, M., B. von Laufenberg, E. Schmidt and M. Colombet (2018), "Re-Entrainment of Fission Products from Water Pools at Elevated Temperature with Reduced Surface Tension", Test WH-28, Technical Report 1501516 – TR – WH-28, Becker Technologies GmbH, Eschborn, Germany, December 2018.

Freitag, M. and M. Sonnekalb (2018), "Comparison Report for Blind and Open Simulations of HR-49. Passive autocatalytic recombiner operation under counter current flow conditions", Report No. 1501516-CR-HR49, Becker Technologies GmbH, Eschborn, Germany, April 2018.

Freitag, M., E. Schmidt and G. Langer (2019), "Hydrogen Combustion and Flame Propagation in Two-compartment system – Test series HD-40 to HD-45", Report No. 1501516-TR-HD40-HD45, Becker Technologies GmbH, Eschborn, Germany, January 2019.

Freitag, M., E. Schmidt, A. Kühnel, M. Colombet and B. von Laufenberg (2019), "Aerosol Resuspension and Thermal Decomposition by Hydrogen Deflagration - Test HD-46", Technical Report No. 1501516 – TR – HD-46, Becker Technologies GmbH, Eschborn, Germany, September 2019.

Freitag, M and M. Sonnenkalb (2019), "Comparison Report for Blind and Open Simulations of HD-44. Hydrogen combustion and flame propagation in two-compartment system with initial convective flow", Report No. 1501516-CR-HD44, Becker Technologies GmbH, Eschborn, Germany, September 2019.

Funke, F., M. Freitag, E. Schmidt, A. Kühnel, G. Langrock and B. von Laufenberg (2018), "Volatile Iodine Release from Boiling Water Pool at Elevated Temperature – Test Iod-32", Technical Report No. 1501516 – TR – Iod-32, Becker Technologies GmbH, Eschborn, Germany, June 2018.

Funke, F., M. Freitag, E. Schmidt, A. Kühnel, G. Langrock and B. von Laufenberg (2019), "Iodine Resuspension from Painted Surfaces by Hydrogen Deflagration - (Test Iod-34)", Technical Report No. 1501516 – TR – Iod-34, Becker Technologies GmbH, Eschborn, Germany, October 2019.

Gupta, S., G. Langer, G. Langrock and F. Funke (2009), "Hydrogen Recombiner Test HR-31 CsI-PAR Interaction", Technical Report 1501326–HR-QLR-5, Becker Technologies GmbH, Eschborn, Germany, September 2009.

Gupta, S., M. Freitag, E. Schmidt, M. Colombet, B. von Laufenberg, A. Kühnel, G. Langer, F. Funke, G. Langrock, et al. (2017), "Ein- und Mehrraumversuche zum Spaltprodukt- und Wasserstoff-Verhalten im Sicherheitsbehälter – THAI-V. Single- and Multi-Compartment Tests on Fission Product and Hydrogen Behaviour in the Containment – THAI-V", Final Report 1501455-FR, Becker Technologies GmbH, Eschborn, Germany, April 2017.

Kanzleiter, T (1992), "Wasserstoff-Deflagrations-Experimente in einer Mehrraum Containment Geometrie (Hx Versuche) / Hydrogen Deflagration Experiments in a Multi-Compartment Containment Geometry (Hx Tests)", Final Report BIeV-R66.985-01 Battelle-Institut, Frankfurt, Germany, November 1992.

Kanzleiter, T. (2009), "Recombiner Tests HR-14 to HR-16. (Tests using a NIS PAR) Areva, AECL and NIS PAR Comparison", Quick Look Report, Hydrogen Reactor Safety Research Project 150 1326 OECD-NEA, THAI Project Report No. 1501326-HR-QLR-4, Becker Technologies GmbH, Eschborn, Germany, October 2009.

Kataoka, I. and M. Ishii (1984), "Mechanistic Modelling of Pool Entrainment Phenomenon", *International Journal of Heat and Mass Transfer*, Vol. 27 (11), pp. 1999–2014, 1984, Elsevier, Amsterdam.

Kupferschmidt, W.C.H., J.B. Buttazoni, G.J. Evans, D.R. Harris, D.R. Greig, G.W. Koroll and G.G. Sanipelli, (1992), "The effects of Steam on the Oxidation of Cesium Iodide Aerosol during Hydrogen Combustion, Advanced containment experiments report", ACE-TR-B8, 1992.

NEA (2016a), *Aerosol and Iodine Issues, and Hydrogen Mitigation under Accidental Conditions in Water Cooled Reactors: Thermal-hydraulics, Hydrogen, Aerosols and Iodine (THAI-2) Project*, OECD Publishing, Paris, www.oecd-nea.org/jcms/pl_19708.

NEA (2016b), *Benchmark Study of the Accident at the Fukushima-Daiichi Nuclear Power Plant (BSAF Project): Phase I Summary Report*, OECD Publishing, Paris, www.oecd-nea.org/jcms/pl_19680/.

NEA (2010), *Hydrogen and Fission Product Issues Relevant for Containment Safety Assessment under Severe Accident Conditions*, OECD Publishing, Paris, www.oecd-nea.org/jcms/pl_18928/.

Nelson, L.S., W.B. Benedick, W. Einfeld, K.P. Guay, G.D. Valdez, J.H. Lee, R. Knystautas, M. Fresko and M. Gaug (1985), "The Behavior of Reactor Core-simulant Aerosols during Hydrogen/Air Combustion", Report SAND85-1817C Sandia National Laboratories, Albuquerque, 1985.

Paul, D.D., D.C. Newman and R.A. Cudnik (1991), "Radionuclide Scrubbing in Water Pools. Volume 2: Gas-liquid Hydrodynamics with Full-scale Downcomers and Horizontal vents", Report EPRI NP-4154-L, Vol. 2, October 1991.

von Rohr, R. (2000), “Einfluss der Naturkonvektion im Sicherheitsbehälter nach einem schweren Kernschmelzunfall auf die kontrollierte Druckentlastung”, REVENT II, Teil 3. ETH Zürich, Abschlußbericht für das Bundesamt für Energie, Dez 2000.

Schmitt, R. E., M. Fiedler, V. Friehmelt and L Wandzilak (1993), “Experimentelle Untersuchung über das Verhalten von CsI bei H_2-Verbrennung”, Final Report BF - R 67.818, Battelle-Institut, Frankfurt, Germany, September 1993.

Annex A. List of project reports

The reports listed below are restricted to the project signatories. However, the Management Board of the THAI Project has agreed that these Quick Look Reports (QLRs) and Technical Reports (TRs) be disclosed for non-signatory NEA countries after 31 June 2023. They may be obtained after this date upon request to the NEA Secretariat.

Project deliveries

Quick Look Reports (QLR)

Freitag, M. and E. Schmidt (2018), "Hydrogen Combustion and Flame Propagation in Two-compartment System", Test series HD-40 – HD-45, Report No QLR- HD-40 – HD-45, Becker Technologies GmbH, Eschborn, Germany, September 2018.

Schmidt, E. and M. Freitag (2016), "Passive Autocatalytic Recombiner Operation under Counter Current Flow Conditions", Test series HR-46 – HR-50, Report No. QLR – HR46-50, Becker Technologies GmbH, Eschborn, Germany, August 2016.

Freitag, M. and E. Schmidt (2017), "Re-Entrainment of Fission Products from Water Pools at Elevated Temperature", Test WH-24, Report No. QLR – WH24, Becker Technologies GmbH, Eschborn, Germany, July 2017.

Freitag, M. and E. Schmidt (2018), "Re-Entrainment of Fission Products from Water Pools at Elevated Temperature with Reduced Surface Tension", Test WH-28, Report No. QLR – WH28, Becker Technologies GmbH, Eschborn, Germany, September 2018.

Freitag, M., E. Schmidt, F. Funke and G. Langrock, (2018), "Volatile Iodine Release from Boiling Water Pool at Elevated Temperature", Test Iod-32, Report No. QLR – Iod32, Becker Technologies GmbH, Eschborn, Germany, Framatome GmbH, Erlangen, Germany, March 2018.

Funke, F., M. Freitag, E. Schmidt, A. Kühnel, G. Langrock and B. von Laufenberg (2019), "Iodine Resuspension from Painted Surfaces by Hydrogen Deflagration", Test Iod-34, Report No.1501516 QLR–Iod-34, Framatome Work Report D02-ARV-01-145-495, Framatome GmbH, Erlangen, Germany, Becker Technologies GmbH, Eschborn, Germany, April 2019.

Freitag, M. et al. (2019), "Aerosol Resuspension and Thermal Decomposition by Hydrogen Deflagration", Test HD-46, Quick Look Report No. 1501516 – QLR – HD-46, Becker Technologies GmbH, Eschborn, Germany, May 2019.

Technical Reports (TR)

Freitag, M., E. Schmidt and G. Langer (2017), "Hydrogen Combustion and Flame Propagation in Two-compartment system", Test series HD-40 to HD-45, Report No. 1501516-TR-HD40-HD45, Becker Technologies GmbH, Eschborn, Germany, January 2019.

Freitag, M. and E. Schmidt (2017), "PAR Operation under Counter Current Flow Conditions", Test series HR-46- HR-50, Technical Report No. 1501516 – TR – HR-46 – HR-50, Becker Technologies GmbH, Eschborn, Germany, June 2017.

Freitag, M., B. von Laufenberg and E. Schmidt (2017), "Re-Entrainment of Fission Products from Water Pools at Elevated Temperature", Test WH-24, Technical Report No. 1501516 – TR – WH-24, Becker Technologies GmbH, Eschborn, Germany, December 2017.

Freitag, M., B. von Laufenberg, E. Schmidt and M. Colombet (2018), 'Re-Entrainment of Fission Products from Water Pools at Elevated Temperature with Reduced Surface Tension", Test WH-28, Technical Report 1501516 – TR – WH-28, Becker Technologies GmbH, Eschborn, Germany, December 2018.

Funke, F. et al (2018), "Volatile Iodine Release from Boiling Water Pool at Elevated Temperature", Test Iod-32, Technical Report No. 1501516 – TR – Iod-32, Becker Technologies GmbH, Eschborn Germany, June 2018.

Funke, F. et al (2019), "Iodine Resuspension from Painted Surfaces by Hydrogen Deflagration", Test Iod-34, Technical Report No. 1501516 – TR – Iod-34, Becker Technologies GmbH, Eschborn, Germany, October 2019.

Freitag, M. et al (2019), "Aerosol Resuspension and Thermal Decomposition by Hydrogen Deflagration", Test HD-46, Technical Report No. 1501516 – TR – HD-46, Becker Technologies GmbH, Eschborn, Germany, September 2019.

Final project report

Gupta, S., G. Poss, M. Freitag, E. Schmidt, M. Colombet, B. von Laufenberg, A. Kühnel, G. Langer, F. Funke and G. Langrock, (2020), "Fission product behaviour, hydrogen mitigation, and hydrogen combustion in water cooled reactors under severe accident conditions", OECD/NEA THAI-3 Project Final Report No. 1501516–FR-1 (Restricted Version), Becker Technologies GmbH, Eschborn, Germany, March 2020.